

Supporting Information
Fabrication of Polythiophene Supported Ag@Fe₃O₄ Nanoclusters and their Utilization as Photocatalyst in Dehydrogenative Coupling Reactions

Radhika Chopra, Manoj Kumar and Vandana Bhalla*

*Department of Chemistry, UGC-Centre for Advanced Studies-II, Guru Nanak Dev University,
Amritsar-143005, Punjab (India)*

Email: vanmanan@yahoo.co.in

Contents (Page: PS1-S49; Table: Table S1-S7; Figure: Figure S1-S50; Scheme: Scheme S1-S4)

Page No. Contents

S5-S9 General Experimental methods

S10 Comparison of wet chemical method in present manuscript over other reported procedure in the Literature for the preparation of Ag@Fe₃O₄ nanocomposites

S11 Scheme showing comparison of generation of Ag@Fe₃O₄ nanocomposites with previously reported methods.

S12 Comparison of catalytic activity of polythiophene supported Ag@Fe₃O₄ nanoclusters (NCs) with other catalytic systems reported in literature for C-H functionalization/C-N bond formation.

S13 UV-Vis spectrum of compound **3** in pure THF and absorption spectra showing the variation of absorbance of compound **3** (10 µM) in H₂O-THF mixture with different fractions of H₂O.

S14 Absorption spectra of compound **3** in H₂O-THF (1:1) solvent mixture upon increasing temperature from 25°C to 70°C and fluorescence spectra of compound **3** (10 µM) in H₂O-THF mixture with different water fractions.

S15 TEM image of compound **3** in H₂O-THF (1:1) mixture showing irregular shaped assemblies and DLS studies of compound **3** in H₂O-THF (1:1) mixture.

S16 UV-vis spectra of compound **3** (10 µM) upon addition of Ag⁺ ions (100 equiv.) with time in H₂O-

THF (1:1) solvent mixture showing surface plasmon resonance (SPR) band at 438 nm and graphical representation of the rate of formation of silver nanoparticles (AgNPs) stabilized by assemblies of compound **3**.

- S17** UV-vis spectra of compound **3** (10 μ M) upon addition of Fe^{3+} ions (20 equiv.) in H_2O -THF (1:1) solvent mixture.
- S18** Absorption spectra of compound **3** (10 μ M) upon addition of various metal ions (Ag^+ , Fe^{3+} , Hg^{2+} , Co^{2+} , Fe^{2+} , Li^+ , Mg^{2+} , Cu^{2+} , Cd^{2+} , Ni^{2+} , Pb^{2+} , Na^+ , K^+ , Zn^{2+} , Al^{3+} , Ca^{2+} and Pd^{2+}) as their perchlorate/nitrate/chloride salt in H_2O -THF (1:1) solvent mixture.
- S19** TEM image showing the (A) formation of $\text{Ag}:\text{Fe}_3\text{O}_4$ NPs prepared by mixing AgNPs and Fe^{3+} ions in 1:1 ratio; (B) formation of $\text{Ag}@\text{Fe}_3\text{O}_4$ NCs by mixing AgNPs and Fe^{3+} ions in 1:2 ratio and UV-vis spectra of aqueous solution of (a) Fe_3O_4 NCs (b) AgNPs (c) $\text{Ag}@\text{Fe}_3\text{O}_4$ NCs stabilized by assemblies of compound **3**.
- S20** Schematic illustration of generation of polythiophene **4** supported $\text{Ag}@\text{Fe}_3\text{O}_4$ NCs (supported by TEM image) by adding aqueous solution of Fe^{3+} ions and AgNPs to the assemblies of compound **3** under stirring and UV-vis spectra with time for simultaneous addition of aqueous solution of Fe^{3+} ions and AgNPs to the assemblies of compound **3** (10 μ M).
- S21** Graphical representation of rate of formation of $\text{Ag}@\text{Fe}_3\text{O}_4$ NCs and fluorescence spectra of compound **3** (10 μ M) with addition of AgNPs and Fe^{3+} ions in H_2O -THF (1:1) solvent mixture
- S22** Cyclic voltammogram of the compound **3** & polythiophene **4** supported $\text{Ag}@\text{Fe}_3\text{O}_4$ NCs in $\text{H}_2\text{O}:\text{CH}_3\text{CN}$ (1:1) solvent mixture and table showing oxidation and reduction potential of compound **3** and polythiophene **4** supported $\text{Ag}@\text{Fe}_3\text{O}_4$ NCs.
- S23** TEM image, SAED pattern and DLS studies of polythiophene **4** supported $\text{Ag}@\text{Fe}_3\text{O}_4$ NCs.

- S24** X-Ray diffraction pattern and Raman scattering spectrum of polythiophene **4** supported Ag@Fe₃O₄ NCs.
- S25** XPS analysis of polythiophene **4** supported Ag@Fe₃O₄ NCs and thermogravimetric analysis (TGA) of compound **3** & polythiophene **4** supported Ag@Fe₃O₄ NCs.
- S26** Hysteresis loop of polythiophene nanosheets supported Ag@Fe₃O₄ nanocomposites at room temperature (25°C) and table showing the coercivity, magnetization values obtained from hysteresis loop of polythiophene nanosheets supported Ag@Fe₃O₄ nanocomposites at room temperature.
- S27** FT-IR Spectrum of compound **3** & polythiophene **4** supported Ag@Fe₃O₄ NCs and ESI-MS spectrum of trimer of oxidized species **4**.
- S28** Schematic illustration for preparation of AgNPs in presence of assemblies of compound **3** and schematic presentation describing the preparation of polythiophene **4** supported Ag@Fe₃O₄ NCs.
- S29** TEM image showing the formation of Ag@Fe₃O₄ NPs prepared by mixing AgNPs & Fe³⁺ ions in 2:1 ratio in presence of assemblies of compound **3**, fluorescence spectra of oxidized species **4** in H₂O-THF (1:1) solvent mixture upon addition of bare Ag@Fe₃O₄ nanocomposites and spectral overlap of absorption spectrum of Ag@Fe₃O₄ NCs & fluorescence spectrum of oxidized species **4** in H₂O-THF (1:1) mixture showing energy transfer from oxidized species **4** to Ag@Fe₃O₄ NCs.
- S30** UV-vis spectra of aqueous solution of (a) bimetallic Ag:Fe₃O₄ NPs (b) AgNPs (c) Fe₃O₄ NCs stabilized by assemblies of compound **5**, TEM image of Ag:Fe₃O₄ NPs stabilized by assemblies of compound **5** and table showing optimization of reaction conditions for dehydrogenative coupling of **6a** utilizing polythiophene **4** supported Ag@Fe₃O₄ NC as photocatalyst.
- S31** Table showing Influence of the stabilizing agent on the photocatalytic efficiency of Ag@Fe₃O₄ nanocomposites in dehydrogenative coupling of phenylhydrazones and structure of polythiophene

S32 Polythiophene supported Ag@Fe₃O₄ NCs (a) separated aqueous layer after completion of model reaction; (b) a magnetic stirring bar put towards the aqueous layer; (c) an external magnet attracted Ag@Fe₃O₄ NCs and recyclability of polythiophene **4** supported Ag@Fe₃O₄ NCs as photocatalyst for synthesis of indazole compounds.

S33 Table showing effect of addition of TEMPO on dehydrogenative coupling of benzophenone phenylhydrazone, **6a** in presence of polythiophene **4** supported Ag@Fe₃O₄ NCs as photocatalyst and mass spectrum of **6a-TEMPO** adduct.

S34 Plausible mechanism for dehydrogenative coupling of **6a** utilizing polythiophene **4** supported Ag@Fe₃O₄ NCs as photocatalyst.

S35-44 NMR spectra of compounds **7a-7j**

S45 NMR spectrum of compound **3**

S46 Mass spectrum of compound **3**

S47 NMR spectrum of compound **5**

S48 Mass spectrum of compound **5**

General experimental methods¹

“UV-vis spectra were recorded on a SHIMADZU UV-2450 spectrophotometer using a quartz cuvette (path length, 1 cm). The fluorescence spectra were obtained with a SHIMADZU 5301 PC spectrofluorimeter. TEM images were recorded in Transmission Electron Microscope (TEM-JEOL 2100F). X-ray diffraction patterns were collected using Rigaku Xpert Pro-X-ray diffractometer provided with CuK α radiation (1.541 Å) in the 2 θ range of 20-80° at a step size of 0.02°. The dynamic light scattering (DLS) data were recorded with MALVERN Instruments (Nano-ZS). Infrared spectra were obtained on Varian 660-IR spectrometer using KBr pellets.” X-ray photoelectron spectra (XPS) were acquired in PHI Versa Prob 5000. The amount of Ag and Fe in catalyst was determined by atomic absorption spectrophotometer (GBC Avant Ver 1.31). Sample preparation was done by reflux assisted digestion of 2 mg of catalyst with concentrated HNO₃. The resulting solution was cooled, centrifuged and filtered. The filtrate was diluted to 10 times with deionized water. The surface area studies were carried out on a Brunauer-Emmett-Teller (BET) surface area analyzer. The samples were degassed at 120°C for 6h in vacuum before taking the measurements. Cyclic Voltammetry studies were performed on CH Instruments CH1660D in presence of supporting electrolyte 0.1M tetrabutylammonium perchlorate (Bu₄NClO₄), Ag/AgCl as reference electrode, platinum wire as counter electrode and glass carbon electrode as working electrode. “TEM and HR-TEM images were recorded using HR-TEM-JEM 2100 microscope.” Raman spectrum was obtained through Renishaw in *via* reflex micro Raman microscope. “To record FT-IR spectra, VARIAN 660 IR Spectrometer was used.” Thermogravimetric analysis (TGA) was carried out on EXSTAR TG/DTA 3600 at a heating rate of 100°C/min under nitrogen atmosphere. VSM measurements were obtained on PAR vibrating sample magnetometer. “Photocatalytic experiments were carried out by using the 100 W tungsten filament bulbs as irradiation source.” Elemental analysis (C, H, and S) was performed on a Flash EA 1112

CHNS analyzer (Thermo Electron Corp.). ^1H NMR was recorded on a JEOL-FT NMR-AL 400 MHz and Bruker (Avance II) FT-NMR 500 MHz spectrophotometer using CDCl_3 as solvent and tetramethylsilane ($\text{Si}(\text{CH}_3)_4$) for internal standards. Further, NMR data was expressed as follows: chemical shifts in ppm (δ) and coupling constants in Hz (J). Multiplicities of signals were quoted as follows: s = singlet, d = doublet, dd = doublet of doublet, t = triplet, dt = doublet of triplet and m = multiplet.

Quantum Yield Calculations:

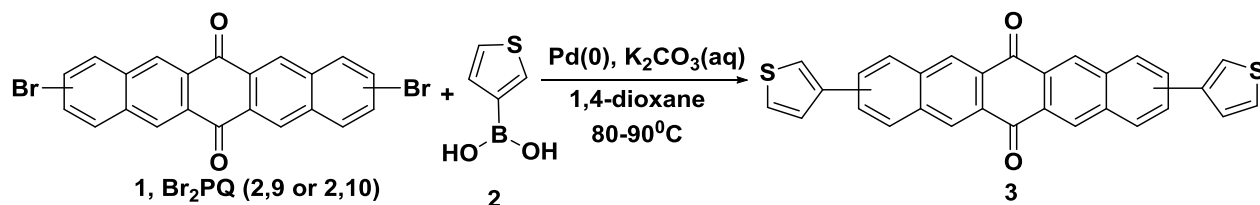
To find out the fluorescence quantum yield of compound **3**, solution of diphenylanthracene ($\Phi_{\text{fr}} = 0.90$ in cyclohexane) was used as reference at an excitation wavelength (λ_{ex}) of 322 nm. Further, the following equation was used to determine the quantum yield:

$$\Phi_{\text{fs}} = \Phi_{\text{fr}} \times \frac{1-10^{-A_{\text{rLr}}}}{1-10^{-A_{\text{sLr}}}} \times \frac{N_{\text{s}}^2}{N_{\text{r}}^2} \times \frac{D_{\text{s}}}{D_{\text{r}}}$$

Φ_{fs} and Φ_{fr} signify the fluorescence quantum yields of sample and reference, respectively. L_{s} , A_{s} , D_{s} and N_{s} are the length of the absorption cells, absorbance, respective areas of emission and refractive index of sample, respectively. L_{r} , A_{r} , D_{r} and N_{r} are the length of the absorption cells, absorbance, respective areas of emission and refractive index of reference, respectively.

EXPERIMENTAL SECTION

Synthetic scheme of compound **3**:

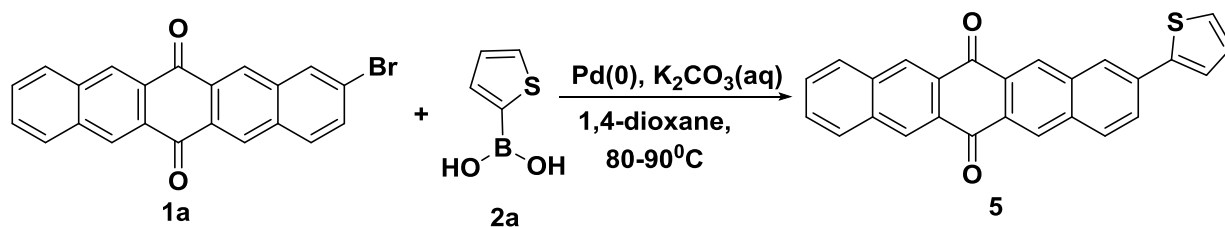


Scheme S1 Synthesis of pentacenequinone compound **3**

To a mixture of compounds **1** (0.30 g, 0.64 mmol) and **2** (0.17 g, 1.35 mmol) in 20 mL of 1, 4-dioxane was added 1 mL of aqueous solution of K_2CO_3 (0.71 g, 5.15 mmol) followed by addition of $[\text{Pd}(\text{PPh}_3)_4]$ (0.16 g, 0.14 mmol) under N_2 atmosphere (Scheme S1). The reaction mixture was refluxed

for 24 h. After completion of the reaction, the excess solvent was removed under reduced pressure and the residue so obtained was dissolved in DCM. The organic layer was washed with water, dried over anhydrous Na₂SO₄, and removed under reduced pressure to give a crude product which was purified by column chromatography using chloroform/hexane (7:3) as an eluent to afford compound **3** as yellow solid (0.18 g in 60% yield); mp: >280°C. ¹H NMR (500 MHz, CDCl₃) δ = 8.98 (s, 2H), 8.95 (s, 2H), 8.32 (s, 2H), 8.17 (d, *J* = 8.5 Hz, 2H), 7.99 (d, *J* = 8.5 Hz, 2H), 7.74-7.71 (m, 2H), 7.61-7.58 (m, 2H), 7.53-7.50 (m, 2H) ppm; *m/z* = 473.2387 [M + H]⁺; Elemental analysis: Calcd. For C₃₀H₁₆O₂S₂: C 76.25; H 3.41; S 13.57. Found: C 76.23; H 3.40; S 13.54. IR (KBr): ν_{max} (in cm⁻¹) = 3092 (C-H_a stretching), 1685(s), 1612(s), 1577(s) and 890 (C-H_a out of plane bending). The ¹³C NMR spectrum of compound **3** could not be recorded due to its poor solubility.

Synthetic scheme of compound **5**:



Scheme S2 Synthesis of pentacenequinone compound **5**

To a mixture of compounds **1a** (0.30 g, 0.78 mmol) and **2a** (0.11 g, 0.85 mmol) in 20 mL of 1,4-dioxane was added 1 mL of aqueous solution of K₂CO₃ (0.86 g, 6.2 mmol) followed by addition of [Pd(PPh)₃]₄ (0.27 g, 0.23 mmol) under nitrogen atmosphere (Scheme S2). The reaction mixture was refluxed for 24 h under N₂ atmosphere. After completion of the reaction, the excess solvent was removed under reduced pressure. The residue so obtained was dissolved in DCM. The organic layer was washed with water, dried over anhydrous Na₂SO₄, and removed under reduced pressure to give a crude product which was purified by column chromatography using chloroform/hexane (4:6) as an eluent to afford compound **5** as yellow solid (0.19 g in 63% yield); mp: >280°C. ¹H NMR (500 MHz,

CDCl_3) δ = 8.96 (s, 2H), 8.95 (s, 1H), 8.93 (s, 1H), 8.32 (s, 1H), 8.15-8.13 (m, 3H), 7.99-7.97 (m, 1H), 7.73-7.71 (m, 2H), 7.57-7.56 (m, 1H), 7.44-7.43 (m, 1H), 7.20-7.18 (m, 1H) ppm; m/z = 413.2716 $[\text{M} + \text{Na}]^+$; Elemental analysis: Calcd. For $\text{C}_{26}\text{H}_{14}\text{O}_2\text{S}$: C 79.98; H 3.61; S 8.21. Found: C 79.96; H 3.59; S 8.19. The ^{13}C NMR spectrum of compound **5** could not be recorded due to its poor solubility.

Synthesis of silver nanoparticles (AgNPs):

The AgNPs were prepared by reducing the AgNO_3 utilizing assemblies of compound **3**. Assemblies of compound **3** were prepared by dissolving compound **3** (10 μM) in H_2O -THF (1:1) solvent mixture. To generate AgNPs, 0.1 M AgNO_3 (300 μL) solution was added to 3 mL of assemblies of compound **3** (1×10^{-4} M). The resulting reaction mixture was stirred at room temperature to obtain greyish AgNPs. These AgNPs were washed with THF and water in order to remove unreacted AgNO_3 and were utilized as such in the fabrication of polythiophene **4** supported $\text{Ag@Fe}_3\text{O}_4$ NCs. The concentration of AgNPs solution was found to be 0.009 M as determined by AAS.

Generation of polythiophene 4 supported $\text{Ag@Fe}_3\text{O}_4$ NCs:

(a) Polythiophene 4 supported $\text{Ag-Fe}_3\text{O}_4$ nanocomposites (1:1)

0.3 mL of AgNPs (0.009 M, dispersed in water) and 0.06 mL of FeCl_3 (0.1 M) solution were simultaneously added to 6 mL of assemblies of compound **3** (10^{-4} M) in H_2O -THF (1:1) solvent mixture with vigorous stirring. During stirring, color of solution was changed from light brown to blackish brown indicating the generation of polythiophene **4** supported $\text{Ag-Fe}_3\text{O}_4$ nanocomposites. Black colored precipitates were observed after stirring the reaction mixture continuously for 1h at room temperature. The resulting reaction mixture was sonicated to obtain homogeneous solution.

(b) Polythiophene 4 supported $\text{Ag@Fe}_3\text{O}_4$ NCs (1:2)

For preparation of polythiophene **4** supported $\text{Ag@Fe}_3\text{O}_4$ NCs (1:2), 0.3 mL of AgNPs solution (0.009 M), 120 μL of FeCl_3 solution (0.1 M) and 9.0 mL of assemblies of compound **3** (10^{-4} M) in H_2O -THF

(1:1) solution were mixed and stirred vigorously at room temperature for 1h. 5.0 mL of this solution was used as such for carrying out dehydrogenative coupling reactions.

(c) Polythiophene 4 supported Ag@Fe₃O₄ NPs (2:1)

For preparation of polythiophene 4 supported Ag@Fe₃O₄ NPs (1:2), 0.6 mL of AgNPs solution (0.009 M), 60 μ L of FeCl₃ solution (0.1 M) and 9.0 mL of assemblies of compound 3 (10⁻⁴ M) in H₂O-THF (1:1) solution were mixed. The resulting solution was vigorously stirred for 1h at room temperature.

General experimental procedure for dehydrogenative coupling reactions utilizing polythiophene 4 supported Ag@Fe₃O₄ NCs (1:2) as photocatalyst:

In a 50 ml round-bottom flask (RBF), benzophenone phenylhydrazone, **6a** (1.0 equiv., 0.1 g) was dissolved in 10 mL of toluene-H₂O (1:1) solvent mixture in presence of *in situ* generated polythiophene 4 supported Ag@Fe₃O₄ nanoclusters (0.01 mmol). After degassing the reaction mixture under vacuum for 2-3 min, the RBF was put in a water bath (to prevent heating effect) on magnetic stirrer. The reaction mixture was irradiated with a 100 W tungsten filament bulb (0.4 W/cm²) to provide visible light for 8 h. After completion of the reaction, solvent was evaporated under reduced pressure and the resulting residue was dissolved in DCM. The organic layer was washed with water, dried over anhydrous Na₂SO₄ and concentrated under reduced pressure to yield the crude product which was recrystallized from ethanol and hexane to obtain pure product, **7a**. The aqueous layer containing photocatalyst was retrieved magnetically and was reused for carrying out further dehydrogenative coupling reactions.

For preparation of indazole derivatives, reactants (**6a-6j**) were synthesized according to previously reported methods².

Table S1. Comparison of wet chemical method in present manuscript over other reported procedure in the literature for the preparation of Ag@Fe₃O₄ nanocomposites.

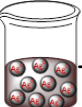
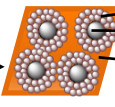
Journal	Nanoparticles	Preparation method	Chemicals used	External Reducing /oxidising agent/Surfactant/Base	Temp (°C)	Time	Application	Shape	Size	Re-cyclability of catalyst
Present work	Polythiophene supported Ag@Fe₃O₄ magnetic nanoclusters	Wet Chemical method	Pentacenequinone compound 3, AgNO₃, FeCl₃·6H₂O	No	Room temperature	4 h	C-N bond formation via Dehydrogenative coupling	Spherical shaped	34 nm	Yes (8 times)
<i>ACS Appl. Mater. Interfaces</i> 2017 , 9, 24433	Ag@Fe ₃ O ₄ core-shell NPs	Solvo thermal method	Fe(NO ₃) ₃ ·9H ₂ O, AgNO ₃ , NaAc, PDDA, ethylene glycol	Yes	210 °C	4 h	-	Spherical shaped	141.4 - 181.2 nm	-
<i>New J. Chem.</i> , 2017 , 41, 10155	Ag@ Fe ₃ O ₄ -PEI NPs	Solvo thermal method	Fe(NO ₃) ₃ ·9H ₂ O, AgNO ₃ , NaAc, PVP	Yes	30-200 °C	8h	Bacterial adsorbent	Spherical shaped	175 nm	Yes (6 times)
<i>ACS Sustainable Chem. Eng.</i> 2016 , 4, 965	Ag-Fe ₃ O ₄ nanoparticles	Coprecipitation route	FeCl ₃ ·6H ₂ O, FeSO ₄ ·7H ₂ O, NaOH, CMC-stabilized Ag NPs	Yes	100 °C	1h	Reduction of aldehydes using 40 bar H ₂	Spherical shaped	17-18 nm	Yes (6 times)
<i>ACS Appl. Mater. Interfaces</i> 2016 , 8, 25162	Ag-Fe ₃ O ₄ Core- Shell	Solvo thermal method	Fe(NO ₃) ₃ ·9H ₂ O, AgNO ₃ , NaOAc	Yes	200 °C	24h	-	Nano flowers	120/210 nm	-
<i>ACS Appl. Mater. Interfaces</i> 2015 , 7, 16027	Ag-Fe ₃ O ₄ Core- Shell	Coprecipitation route	FeCl ₃ ·6H ₂ O, FeCl ₂ ·4H ₂ O, NaOH, PVP, AgNWs	Yes	70 °C	1h	-	Fe ₃ O ₄ nanospheres on AgNWs.	90-143 nm	-
<i>RSC Adv.</i> 2015 , 5, 102610	Ag:Fe ₃ O ₄ nanocomposite	Solvo thermal method	Silver oleate, Iron oleate, octadecylene, Oleic acid	Yes	150 °C	5h	Detection of pesticides in water	Spherical	50 nm	-
<i>Scientific Reports</i> 2014 , 4, 6839	Ag@Fe ₃ O ₄ core-shell nanoparticles	Thermal decomposition	Fe(acac) ₃ , 1,2-hexadecanediol, oleylamine, oleic acid, AgNO ₃	Yes	200-260 °C	2h	-	Brick shaped	13 nm	-
<i>Nanoscale</i> 2014 , 6, 12618	Fe ₃ O ₄ -Ag nanoparticles	Solvo thermal method	AgNO ₃ , Oleic acid sodium oleate, Polyacrylate stabilized Fe ₃ O ₄	Yes	200 °C	8h	Detection of thiram in water	Dumb bell shaped	500 nm	-
<i>Green Chem.</i> 2014 , 16, 2835	Ag-Fe ₃ O ₄ @chitin nanocomposite	Solvo thermal method	FeCl ₂ ·4H ₂ O, NaOH, AgNO ₃ , Chitin	Yes	90 °C	10 h	Reduction of 4-nitrophenol to 4-aminophenol using NaBH ₄	Spherical	10-40 nm	Yes (10 times)
<i>J. Phys. Chem. C</i> 2014 , 118, 13168	Ag-Fe ₃ O ₄	Thermal decomposition	Ag seeds, Fe(acac) ₃ , oleylamine, oleic acid	Yes	300 °C	40 min	-	Nano flowers	7-8 nm	-
<i>J. Mater. Chem. C</i> 2014 , 2, 9964	Ag-Fe ₃ O ₄	Coprecipitation route	FeCl ₃ ·6H ₂ O, FeCl ₂ ·4H ₂ O, NH ₄ OH, PAA, AgNO ₃ , Sodium citrate, NaBH ₄	Yes	RT	2-3 h	Detection of dopamine	Spherical	30 nm	-

Previous work on preparation of Ag@Fe₃O₄ nanocomposites³⁻⁵

- (a) $\text{Fe}(\text{NO}_3)_3 \cdot 9\text{H}_2\text{O} + \text{AgNO}_3 \xrightarrow[200^\circ\text{C}, 6\text{h}]{\text{NaAc, Ethylene glycol, Citric acid}} \text{Ag@Fe}_3\text{O}_4 \text{ nanocomposites}$
Size = 141.4-181.2 nm
- (b) $\text{Fe}(\text{NO}_3)_3 \cdot 9\text{H}_2\text{O} + \text{AgNO}_3 \xrightarrow[200^\circ\text{C}, 24\text{h}]{\text{PVP, NaAc, Ethylene glycol}} \text{Ag@Fe}_3\text{O}_4 \text{ nanocomposites}$
Size = 175 nm
- (c) $\text{Fe}(\text{NO}_3)_3 \cdot 9\text{H}_2\text{O} + \text{AgNO}_3 \xrightarrow[210^\circ\text{C}, 24\text{h}]{\text{NaAc, Ethylene glycol}} \text{Ag@Fe}_3\text{O}_4 \text{ nanocomposites}$
Size = 120/210 nm

- Prolonged reaction time
- High temperature
- Catalytic applications not much explored

Recent approach

- (d) Assemblies of compound 3 + AgNO₃ $\xrightarrow{3\text{h}}$  $\xrightarrow[75 \text{ min.}]{\text{Assemblies of compound 3, FeCl}_3 \cdot 6\text{H}_2\text{O}}$ 
Solution of AgNPs Polythiophene supported Ag@Fe₃O₄ nanoclusters
Size = 34 nm

- Mixed aqueous media
- Room temperature
- Highly efficient recyclable, photocatalyst in C-H to C-N bond transformation.

Scheme S3 Scheme showing comparison of generation of Ag@Fe₃O₄ nanocomposites with previously reported methods.

Table S2 Comparison of catalytic activity of polythiophene supported Ag@Fe₃O₄ nanoclusters with other catalytic systems reported in literature for C-H functionalization/C-N bond formation.

Journal Name	Catalyst	Catalyst loading	Ligand/base/Oxidant	Solvent	Temperature	Time	Yield
Present manuscript	Polythiophene supported Ag@Fe₃O₄ NCs	0.01mmol	-	H₂O:Toluene	Visible light	7-10h	64-90%
<i>Angew. Chem. Int Ed.</i> 2017 , 56, 1120	Acr ⁺ -Mes ClO ₄ ⁻ , Co(dmgH) ₂ PyCl	3 mol%	-	CH ₃ CN	Blue LED (3W) Under nitrogen atmosphere	24h	35-89%
<i>J. Am. Chem. Soc.</i> 2017 , 139, 643.	Pd(OAc) ₂	0.89 mmol	Di(2-pyridyl) ketone, H ₂ O ₂	CH ₃ CN, MeOH, THF or AcOH	60°-80°C	3-12h	82-98%
<i>Angew. Chem. Int. Ed.</i> 2017 , 56, 7449	[RhCp*Cl ₂] ₂	5 mol%	2-methylquinoline, PhCO ₂ Na, Ag ₂ CO ₃	Toluene	90°C Under nitrogen atmosphere	16h	44-88%
<i>Chem. Commun.</i> 2017 , 53, 5744	CuI or Cu(OTf) ₂	10 mol%	PhI(OTFA) ₂	DCE	100°C	10h	32-85%
<i>Org. Lett.</i> 2017 , 19, 914	Pd(CH ₃ CN) ₂ Cl ₂	10 mol%	Chloranil	1,4-dioxane	80°C	24 h	27-98%
<i>Nat. Commun.</i> 2016 , 7, 11188	Ru(bpy) ₃ Cl ₂ .6H ₂ O	2 mol%	TEMPO, K ₂ CO ₃	CHCl ₃	Blue LED (3W)	5-24h	51-86%
<i>J. Am. Chem. Soc.</i> 2016 , 138, 1265	Pd/bis-sulfoxide, Co(salophen)	2.5-5 mol%	DHBQ, TBAA, O ₂	TBME	45°C	72h	52-96%
<i>Org. Lett.</i> 2016 , 18, 3586	Pd(OAc) ₂	10 mol%	O ₂	DMSO/toluene	80°-120°C	24 h	36-95%
<i>J. Org. Chem.</i> 2016 , 81, 2035	Pd(OAc) ₂	20 mol%	Cu(OAc) ₂ , O ₂	DMSO	120°C	8-10h	63-87%
<i>Chem. Eur. J.</i> 2016 , 22, 15669	Ir(ppy) ₂ (dtbbpy)PF ₆	2 mol%	NaClO	1,4-dioxane	White LED (5 W)	1h	45-91%
<i>Chem. Eur. J.</i> 2016 , 22, 4379	Copper(II) 2-ethylhexanoate	20 mol%	Dess-Martin periodinane	DMSO	110°C	1h	70-87%
<i>Chem. Eur. J.</i> 2016 , 22, 6487	Cu(OAc) ₂	15 mol%	Ag ₂ CO ₃	m-Xylene	140°C	24h	68-91%
<i>ACS Catal.</i> 2015 , 5, 4796	[Ir(dFppy) ₂ phen]PF ₆ , Pd(OAc) ₂	10 mol%	Molecular O ₂	DMSO	80°C, Blue LED (7W)	8-16h	75-94%
<i>Org. Chem. Front.</i> 2015 , 2, 51	Pd(OAc) ₂	10 mol%	Ce(SO ₄) ₂ , DMF, MsOH	DCM	120° C	48h	30-74%

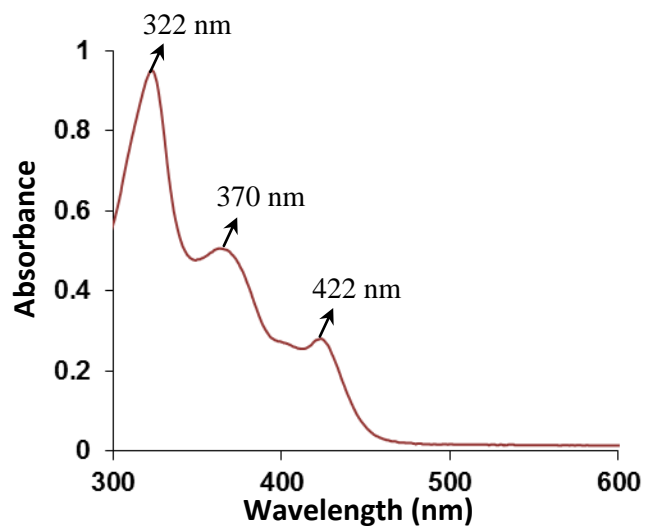


Figure S1 UV-vis spectrum of compound **3** in pure THF.

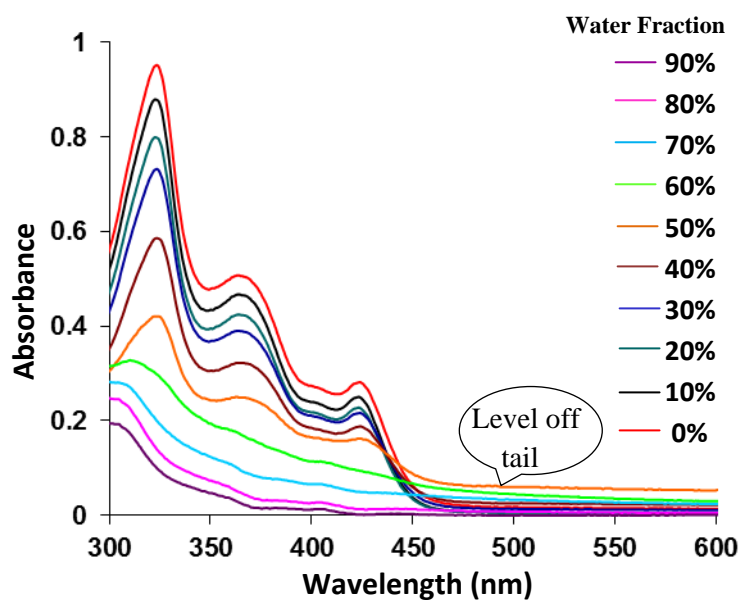


Figure S2 UV-vis spectra showing the variation of absorbance of compound **3** (10 μ M) in H_2O -THF mixture with different fractions of H_2O .

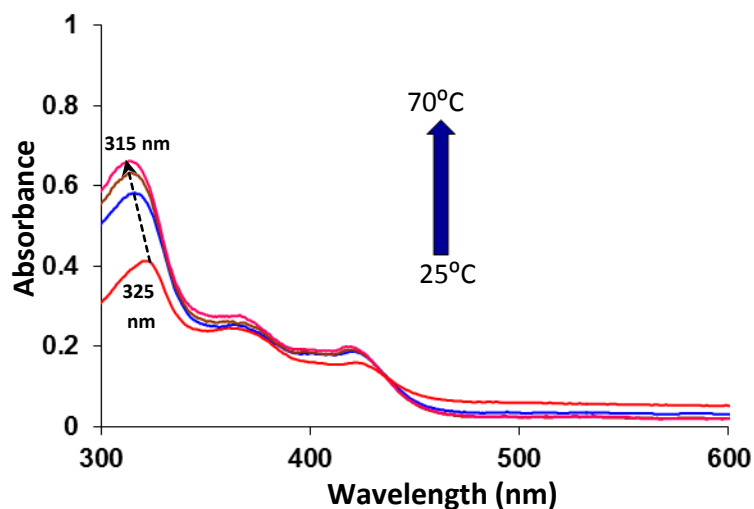


Figure S3 UV-vis absorption spectra of compound **3** in H₂O-THF (1:1) solvent mixture upon increasing temperature from 25 to 70°C.

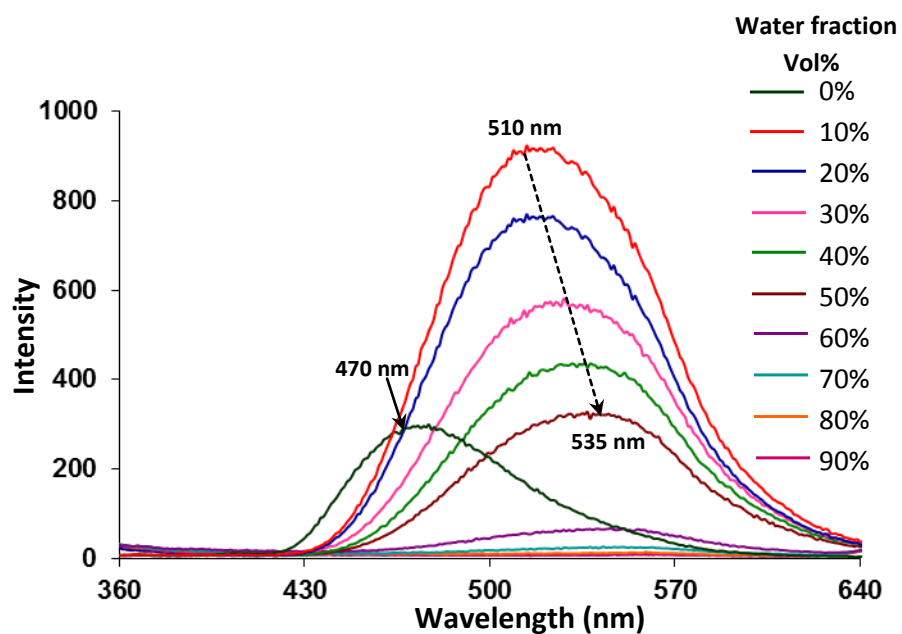


Figure S4 Fluorescence spectra of compound **3** (10 μM) in H₂O-THF mixture with different water fractions; $\lambda_{\text{ex}} = 322$ nm

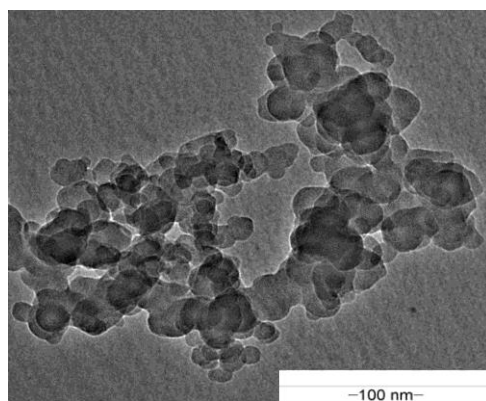


Figure S5 TEM image of compound **3** in H₂O-THF (1:1) mixture showing irregular shaped assemblies; scale bar 100 nm.

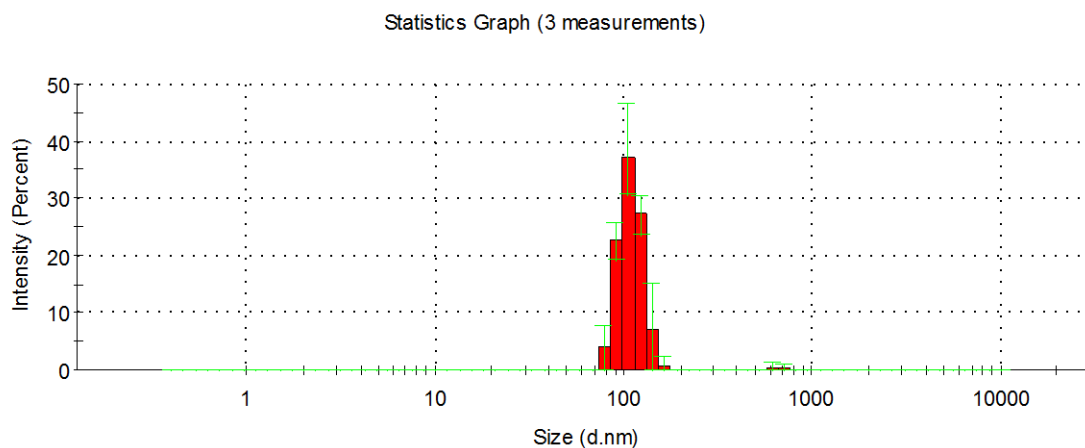


Figure S6 DLS studies of compound **3** in H₂O-THF (1:1) mixture which showed the presence of particles having average diameter in the range of 100 nm.

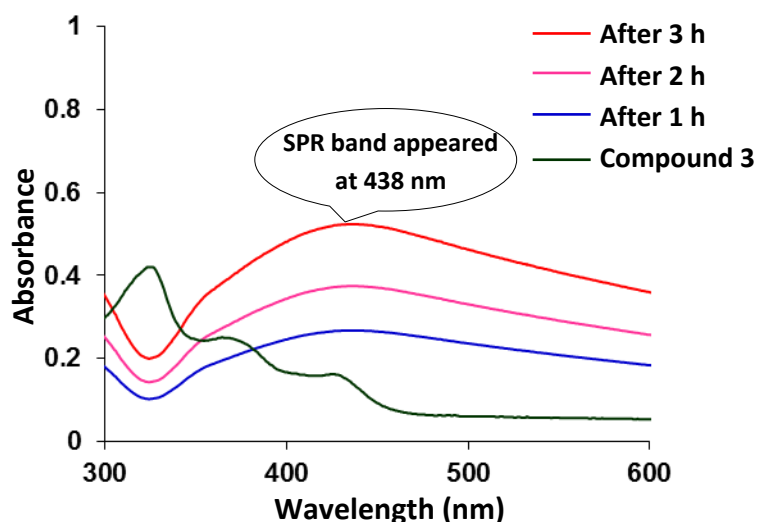


Figure S7 UV-vis spectra of compound **3** (10 μM) upon addition of Ag^+ ions (100 equiv.) with time in H_2O -THF (1:1) solvent mixture showing surface plasmon resonance (SPR) band at 438 nm.

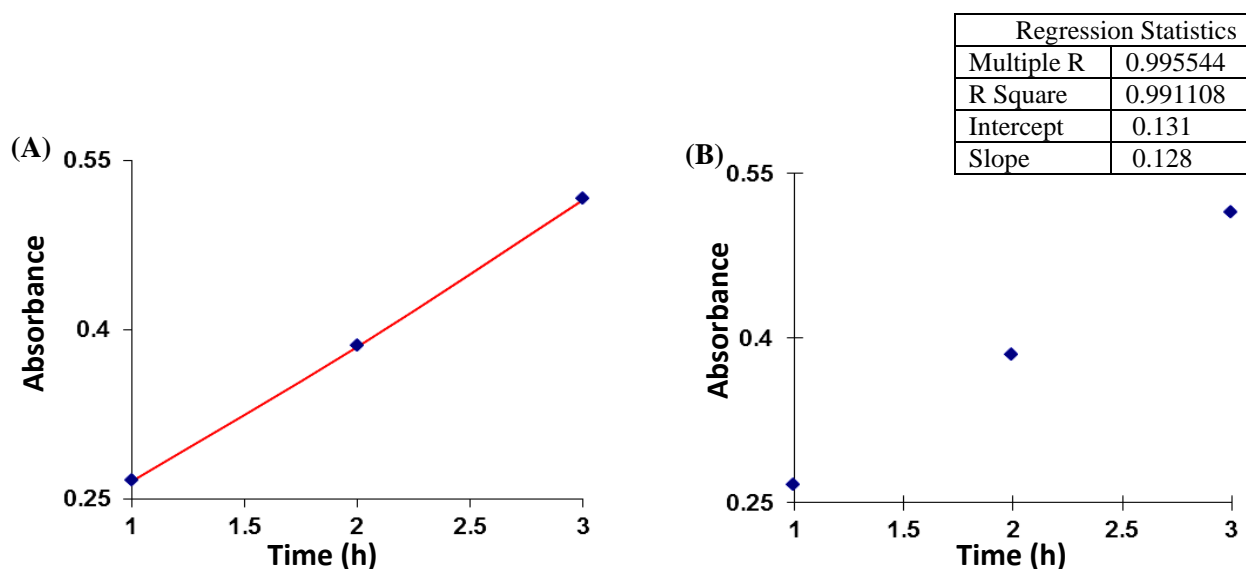


Figure S8 Graphical representation of the rate of formation of AgNPs stabilized by assemblies of compound **3** (A) Time (h) vs. absorbance plot at 438 nm (B) regression plot of A.

The first order⁶ rate constant for the formation of silver nanoparticles was calculated from the changes of intensity of absorbance of assemblies of compound **3** at 438 nm wavelength in the presence of Ag^+ ions at different time interval.⁷⁻⁸ From the time vs. absorbance plot at fixed wavelength 438 nm by using first order rate equation, we get the rate constant = $k = \text{slope} \times 2.303 = 8.18 \times 10^{-5} \text{ sec}^{-1}$.

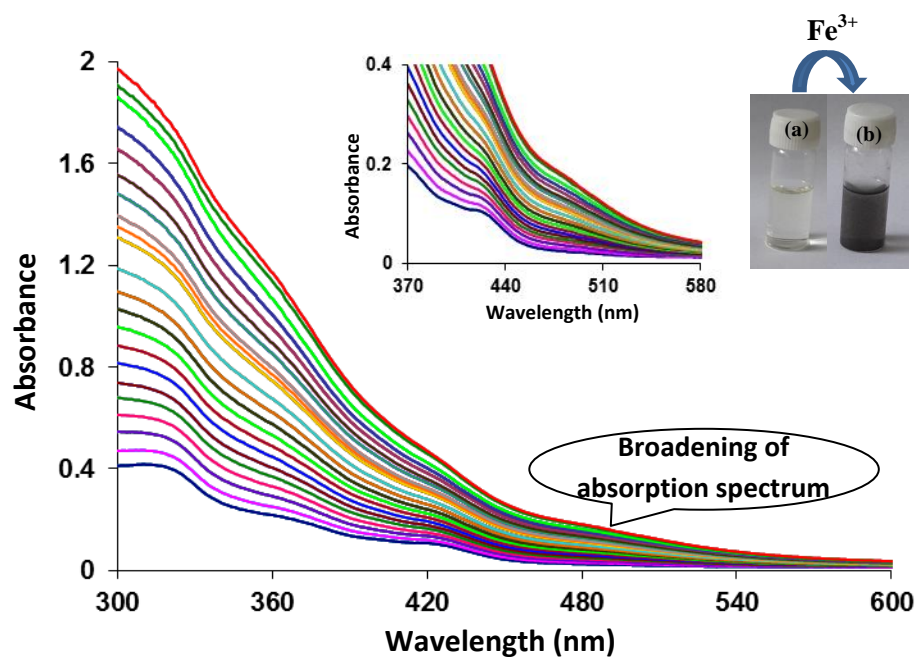


Figure S9 UV-vis spectra of compound **3** (10 μM) upon addition of Fe³⁺ ions (20 equiv.) in H₂O-THF (1:1) mixture; Inset showing enlarged absorption spectra in the range of 370-580 nm along with change in color of solution from colorless to black in presence of Fe³⁺ ions.

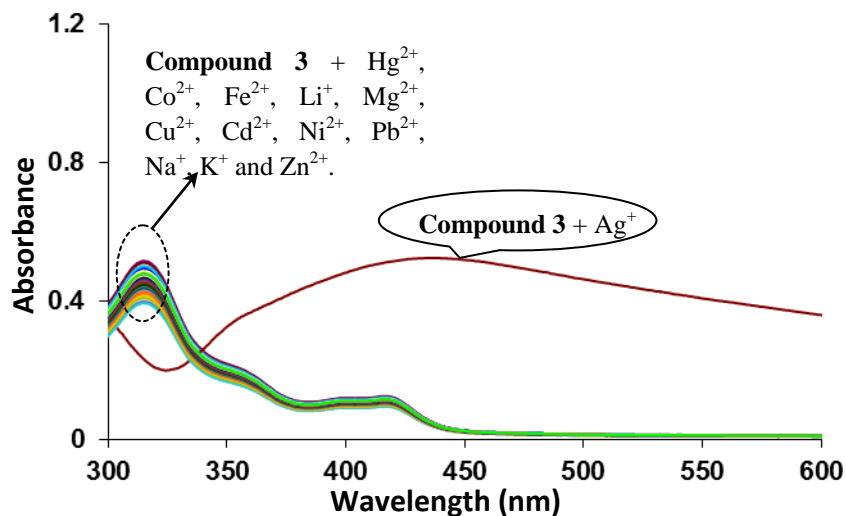


Figure S10 Absorption spectra of compound **3** (10 μM) upon additions of 100 equivalents of various metal ions (Ag^+ , Hg^{2+} , Co^{2+} , Fe^{2+} , Li^+ , Mg^{2+} , Cu^{2+} , Cd^{2+} , Ni^{2+} , Pb^{2+} , Na^+ , K^+ and Zn^{2+}) as their perchlorate/nitrate salt in H_2O -THF (1:1), buffered with HEPES, pH = 7.0.

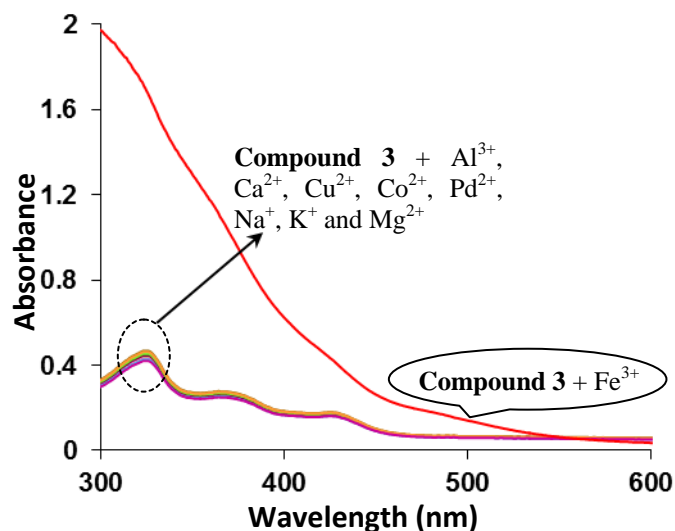


Figure S11 Absorption spectra of compound **3** (10 μM) upon additions of 20 equivalents of various metal ions (Al^{3+} , Ca^{2+} , Cu^{2+} , Co^{2+} , Fe^{3+} , Pd^{2+} , Na^+ , K^+ and Mg^{2+}) as their chloride salt in H_2O -THF (1:1), buffered with HEPES, pH = 7.0.

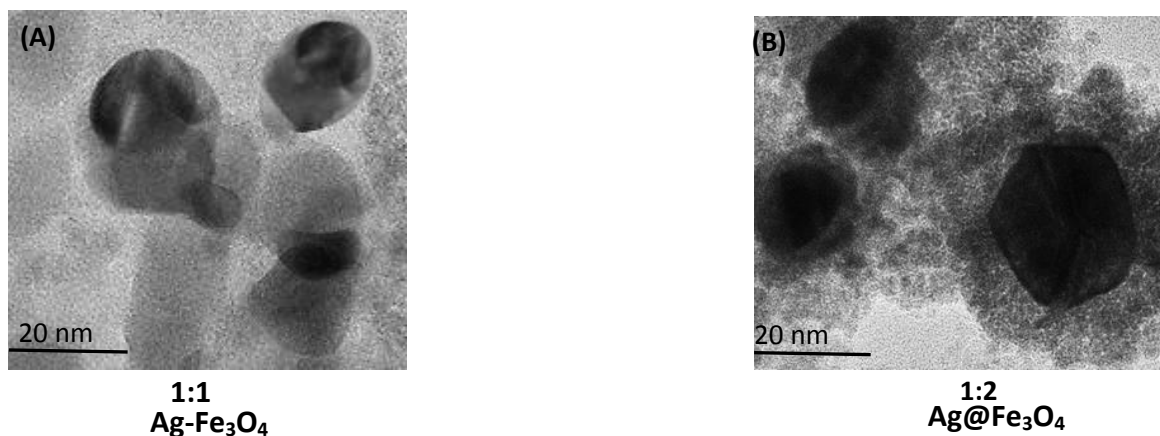


Figure S12 (A) TEM image showing the (A) formation of Ag-Fe₃O₄ NPs prepared by mixing AgNPs and Fe³⁺ ions in 1:1 ratio; (B) formation of Ag@Fe₃O₄ NCs by mixing AgNPs and Fe³⁺ ions in 1:2 ratio.

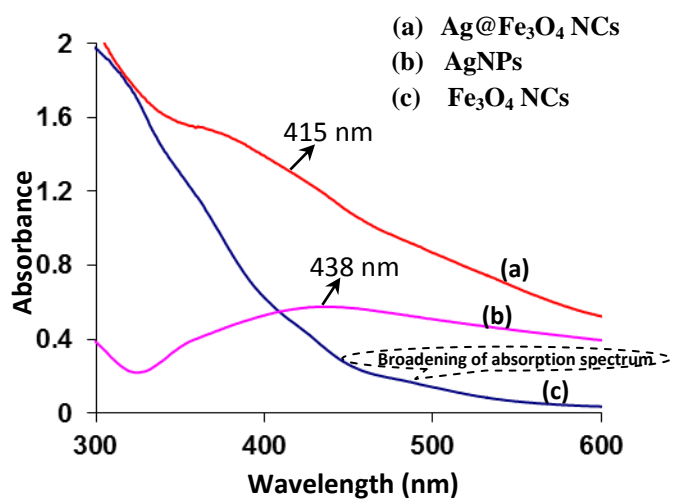


Figure S13 UV-vis spectra of aqueous solution of (a) Fe₃O₄ NCs (b) AgNPs (c) Ag@Fe₃O₄ NCs stabilized by assemblies of compound **3**.

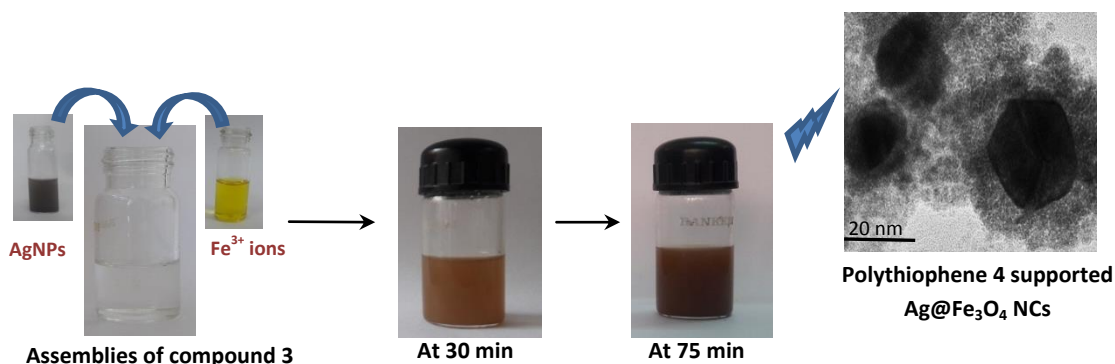


Figure S14 Schematic illustration of generation of polythiophene **4** supported Ag@Fe₃O₄ NCs (supported by TEM image) by adding aqueous solution of Fe³⁺ ions and AgNPs to the assemblies of compound **3** under stirring.

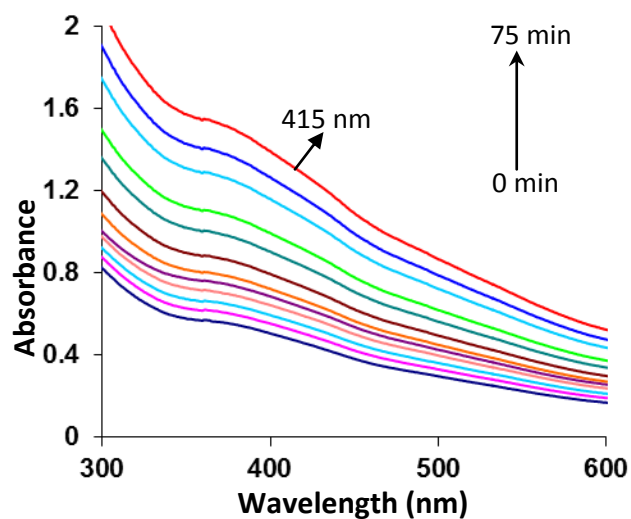


Figure S15 UV-vis spectra with time for simultaneous addition of aqueous solution of Fe³⁺ ions and AgNPs to the assemblies of compound **3** (10 μ M).

Regression Statistics	
Multiple R	0.995065
R Square	0.990155
Intercept	0.443514
Slope	0.010662

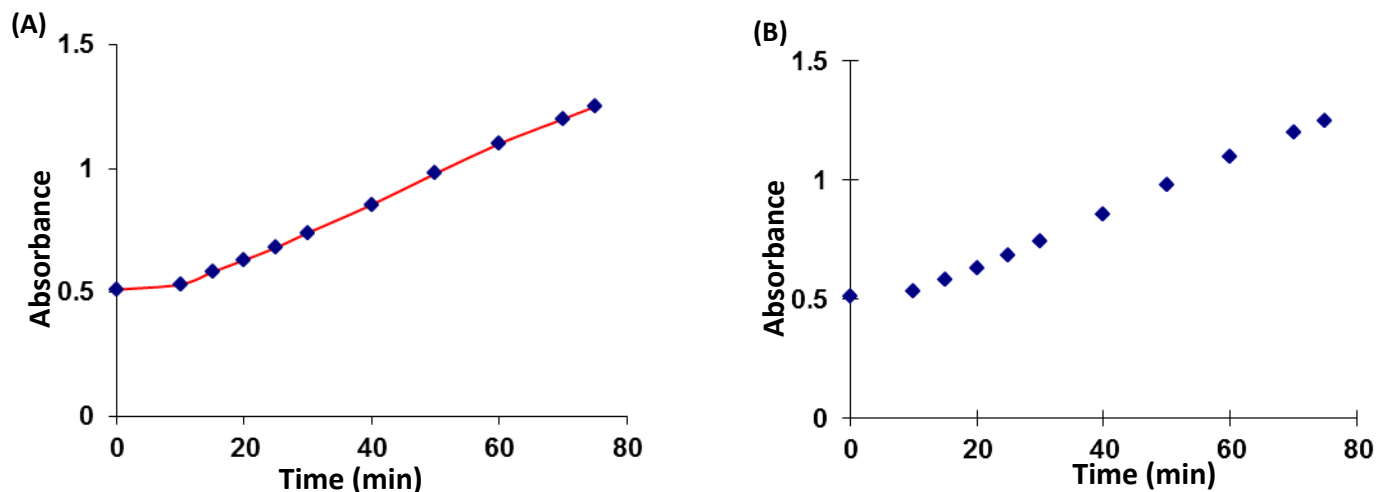


Figure S16 Graphical representation of rate of formation of Ag@Fe₃O₄ NCs (A) Time (min.) vs. absorbance plot at 415 nm (B) regression plot of A.

The first order rate constant for the formation of Ag@Fe₃O₄ NCs was calculated from the change of intensity of blue shifted absorbance band of AgNPs in the presence of assemblies of compound **3** and FeCl₃ solution at different time interval.

From the time vs. absorbance plot at fixed wavelength 415 nm by using first order rate equation, we get the rate constant = $k = \text{slope} \times 2.303 = 4.09 \times 10^{-4} \text{ s}^{-1}$.

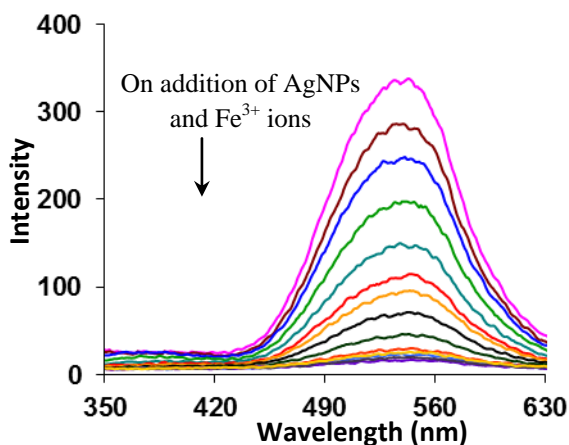


Figure S17 Fluorescence spectra of compound **3** (10 μM) with addition of AgNPs and Fe³⁺ ions in H₂O-THF (1:1) solvent mixture; $\lambda_{\text{ex}} = 322 \text{ nm}$.

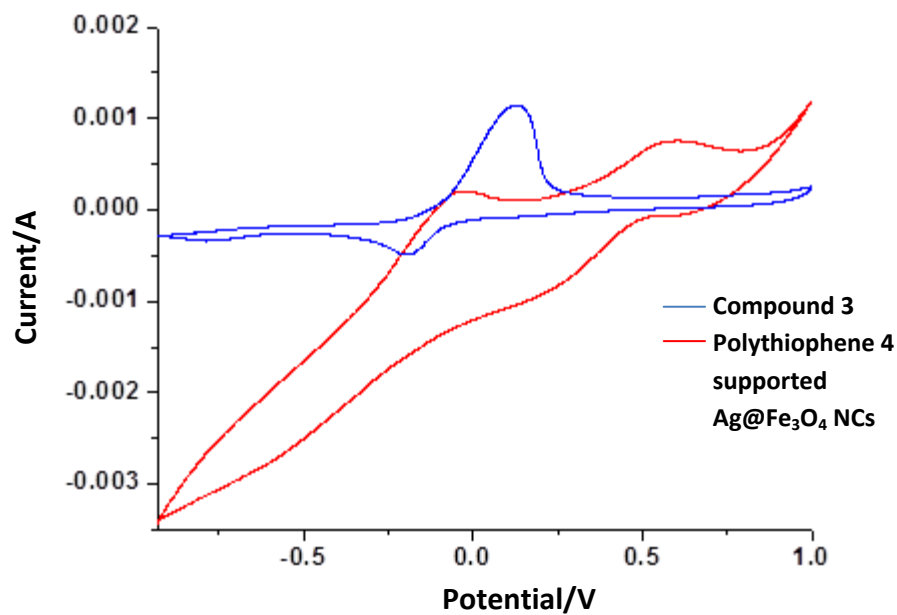


Figure S18 Cyclic voltammogram of the compound **3** and polythiophene **4** supported Ag@Fe₃O₄ NCs in H₂O:CH₃CN (1:1) containing 0.1 M Bu₄NClO₄ (supporting electrolyte) and Ag/AgCl (reference electrode).

Table S3 Table showing oxidation and reduction potential of compound **3** and polythiophene **4** supported Ag@Fe₃O₄ NCs.

Entry	Reduction potential (eV)	Oxidation potential (eV)
Compound 3	-0.19	0.13
Polythiophene 4 supported Ag@Fe ₃ O ₄ NCs	0.22	-0.0787

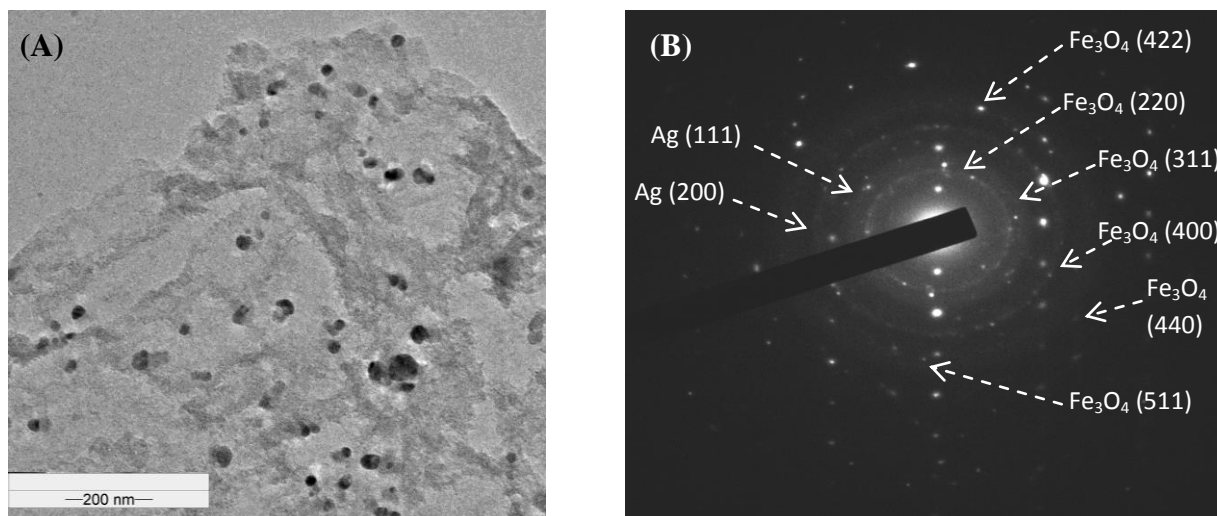


Figure S19 (A) TEM image of polythiophene **4** supported Ag@Fe₃O₄ nanoclusters (B) SAED pattern of polythiophene **4** nanosheets supported Ag@Fe₃O₄ NCs.

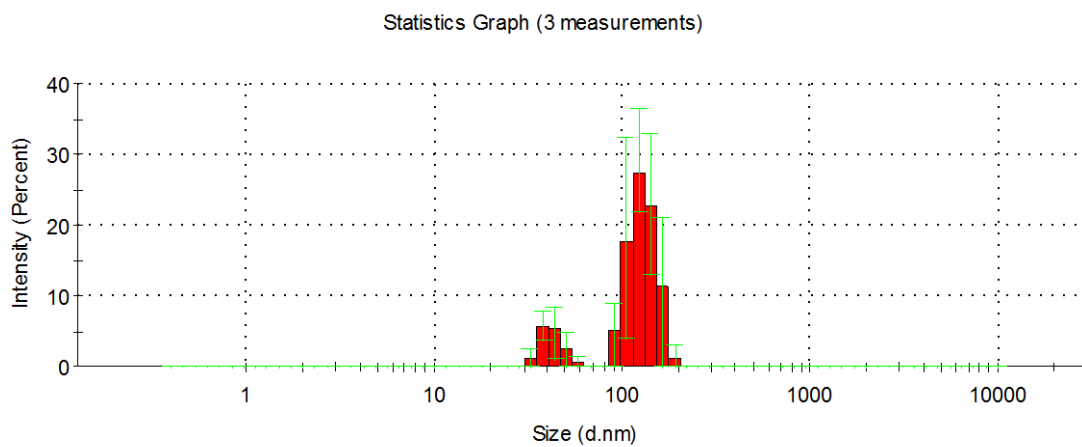


Figure S20 DLS studies of polythiophene **4** supported Ag@Fe₃O₄ nanoclusters indicated the presence of two sets of particles having average size 43 nm and 120 nm.

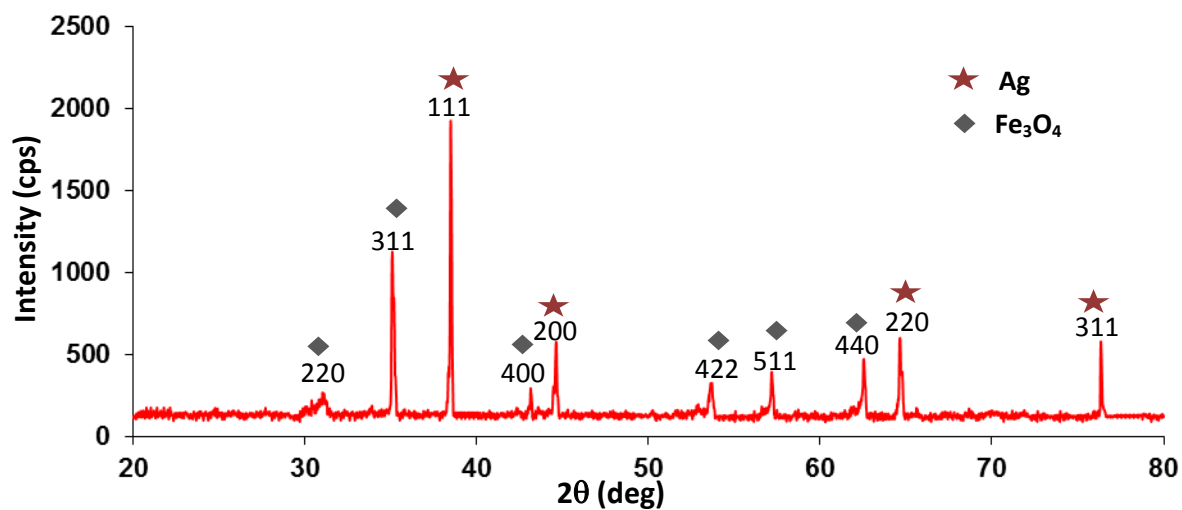


Figure S21 X-Ray diffraction pattern of *in situ* generated $\text{Ag}@\text{Fe}_3\text{O}_4$ NCs.

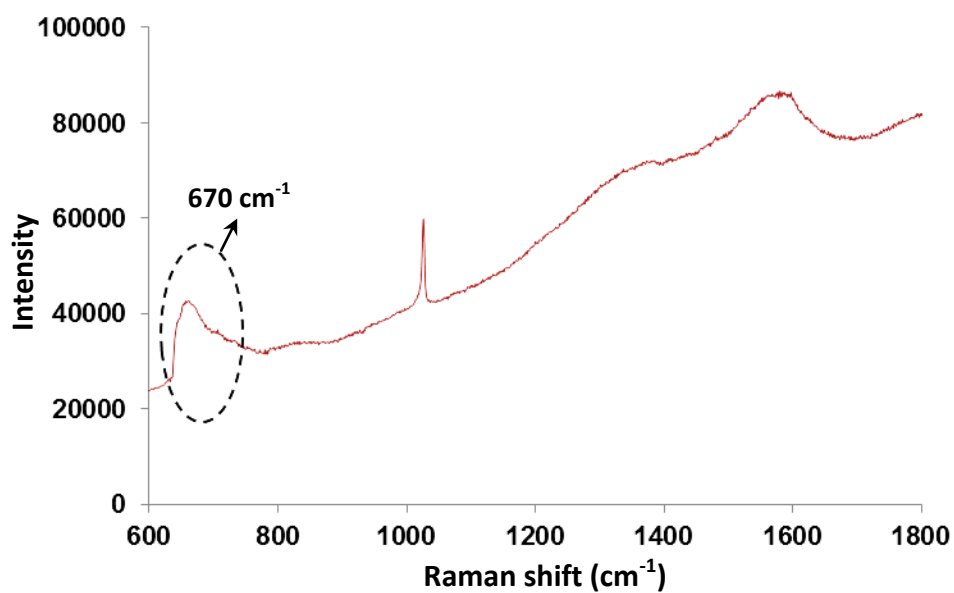


Figure S22 Raman scattering spectrum of polythiophene **4** supported $\text{Ag}@\text{Fe}_3\text{O}_4$ NCs showed the presence of band at 670 cm^{-1} corresponding to the A_{1g} vibration mode of Fe_3O_4 NPs.

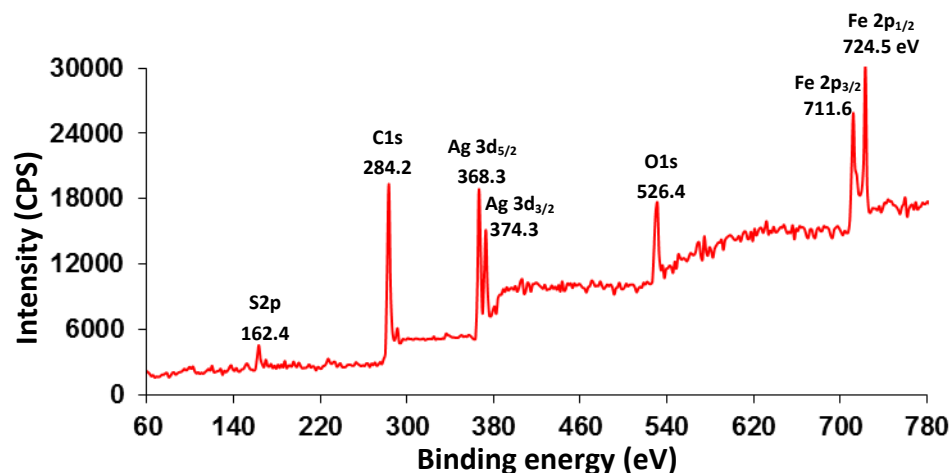


Figure S23 XPS analysis of polythiophene **4** supported Ag@Fe₃O₄ NCs indicated the presence of Ag⁰ and Fe₃O₄ species along with polythiophene.

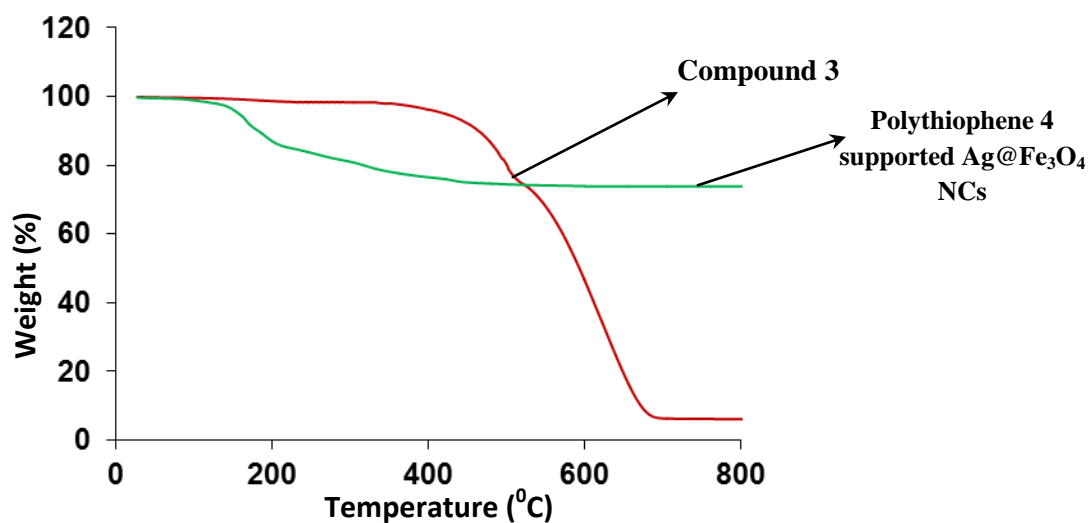


Figure S24 TGA of compound **3** and polythiophene **4** supported Ag@Fe₃O₄ NCs. This data indicated that polythiophene supported Ag@Fe₃O₄ NCs consisted of 28.0 wt% of polythiophene as organic component.

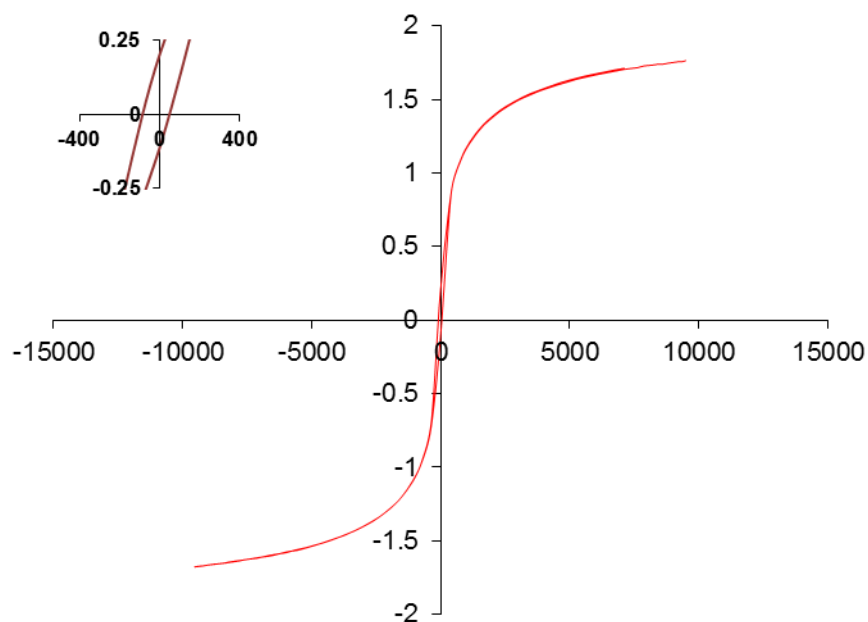


Figure S25 Hysteresis loop of polythiophene **4** supported Ag@Fe₃O₄ nanocomposites at room temperature (25°C). Inset showing expanded curve.

Table S4 Showing the coercivity, magnetization values obtained from Hysteresis loop of polythiophene **4** supported Ag@Fe₃O₄ nanocomposites at room temperature; 25°C.

Parameter	Value	Parameter definition
H _c (Oe)	68.5	Coercive Field: Field at which M/H changes sign
M _r (emu g ⁻¹)	0.177	Remanent Magnetization: M at H=0
M _s (emu g ⁻¹)	40.772	Saturation Magnetization: maximum M measured
S	0.00434	Squareness = M _r /M _s

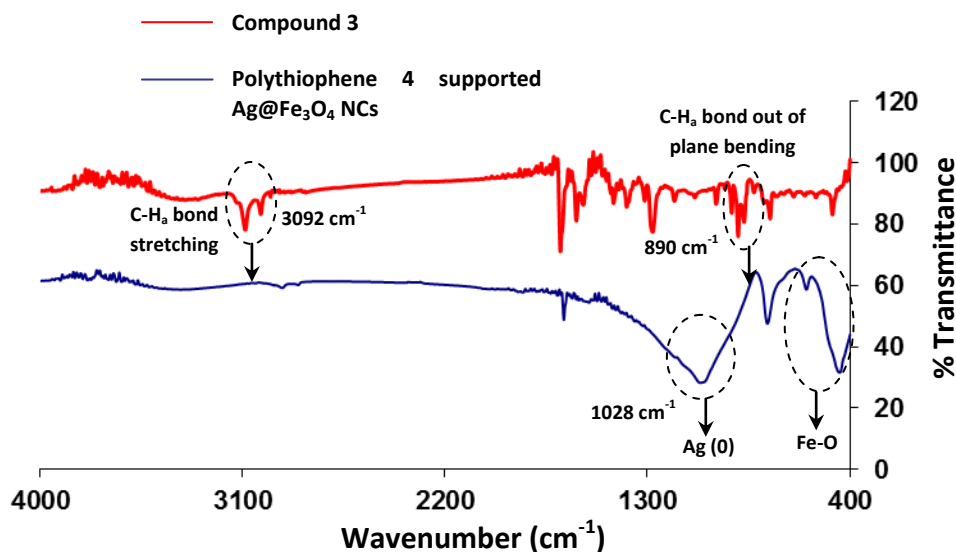


Figure S26 FT-IR spectra of compound **3** and polythiophene **4** supported Ag@Fe₃O₄ NCs showing disappearance of the bands at 3092 and 890 cm⁻¹ indicated the formation of polythiophene species through C-H_a bonds. The peaks in the range of 400-600 cm⁻¹ and 1028 cm⁻¹ are associated with the stretching & torsional vibration modes of the Fe₃O₄ NCs and Ag (0) respectively.

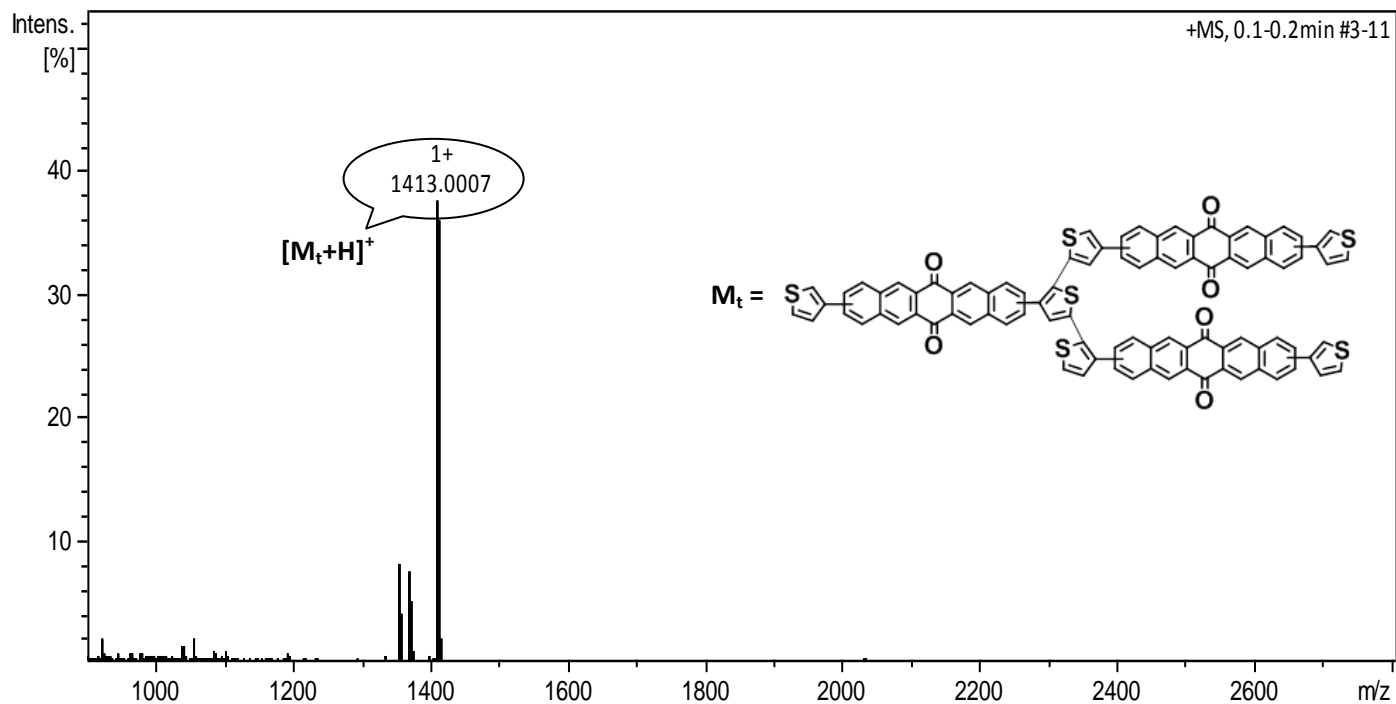


Figure S27 ESI-MS spectrum of trimer formed after oxidation of compound **3** showed a parent ion peak correspond to [M_t+H]⁺, m/z = 1413.0007.

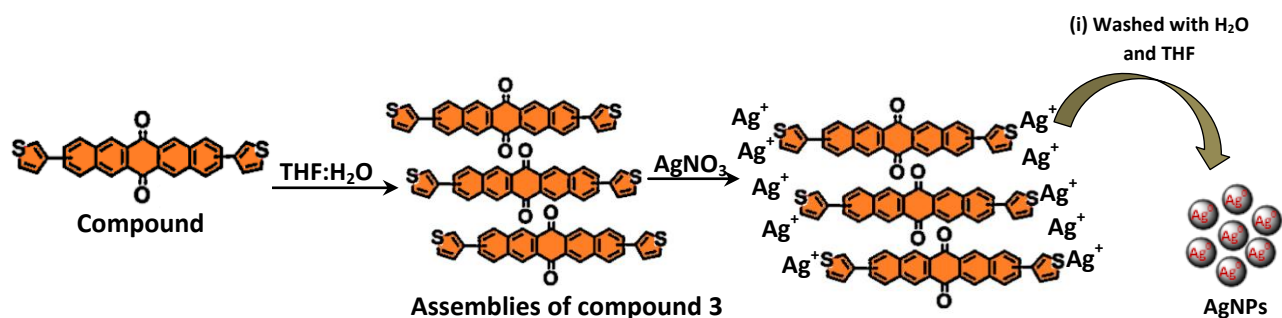


Figure S28 Schematic illustration of preparation of AgNPs in presence of assemblies of compound 3.

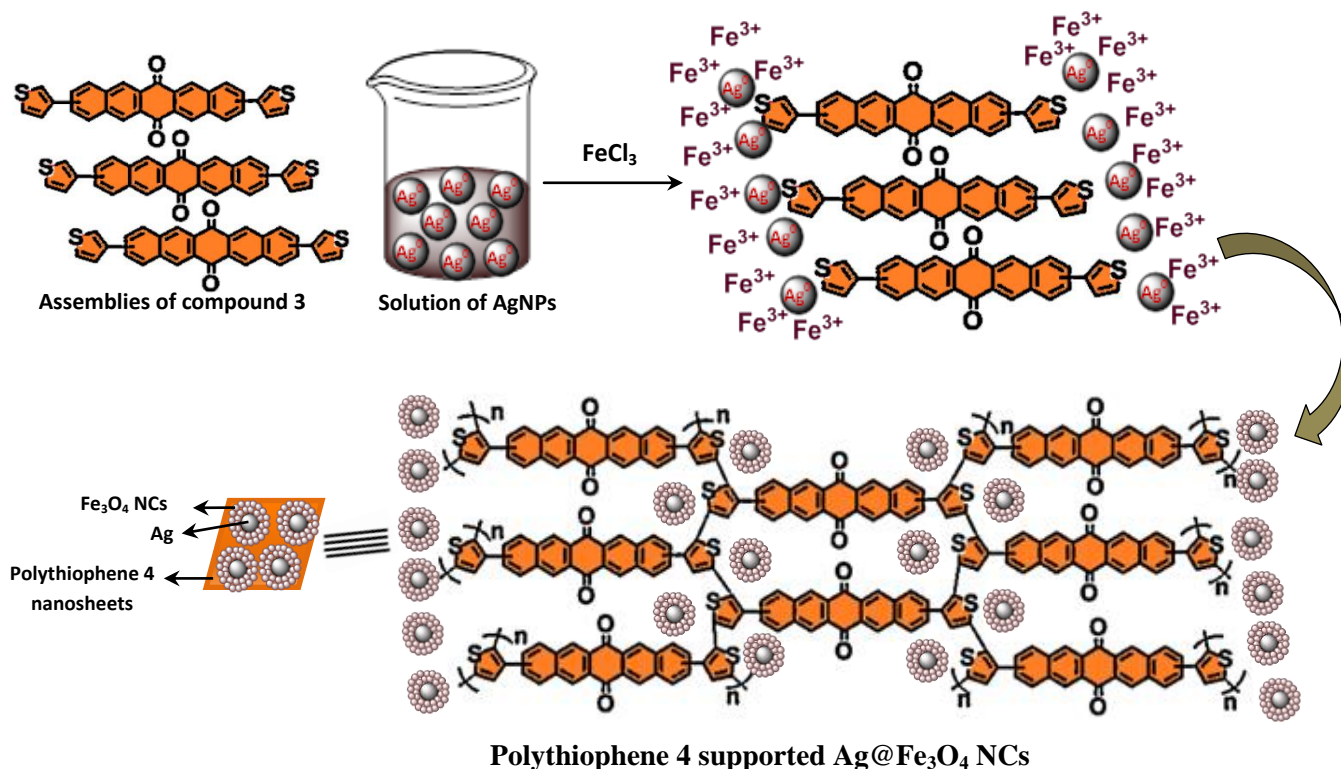
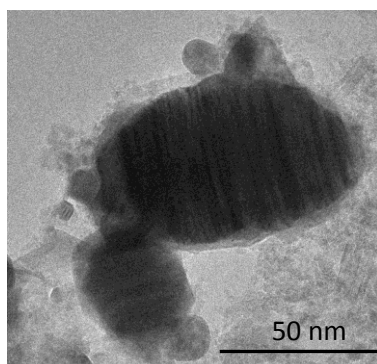


Figure S29 Schematic presentation describing the preparation of polythiophene 4 supported Ag@Fe₃O₄ NCs.



2:1
Ag@Fe₃O₄

Figure S30 TEM image showing the formation of Ag@Fe₃O₄ NPs prepared by mixing AgNPs and Fe³⁺ ions in 2:1 ratio showing larger sized core.

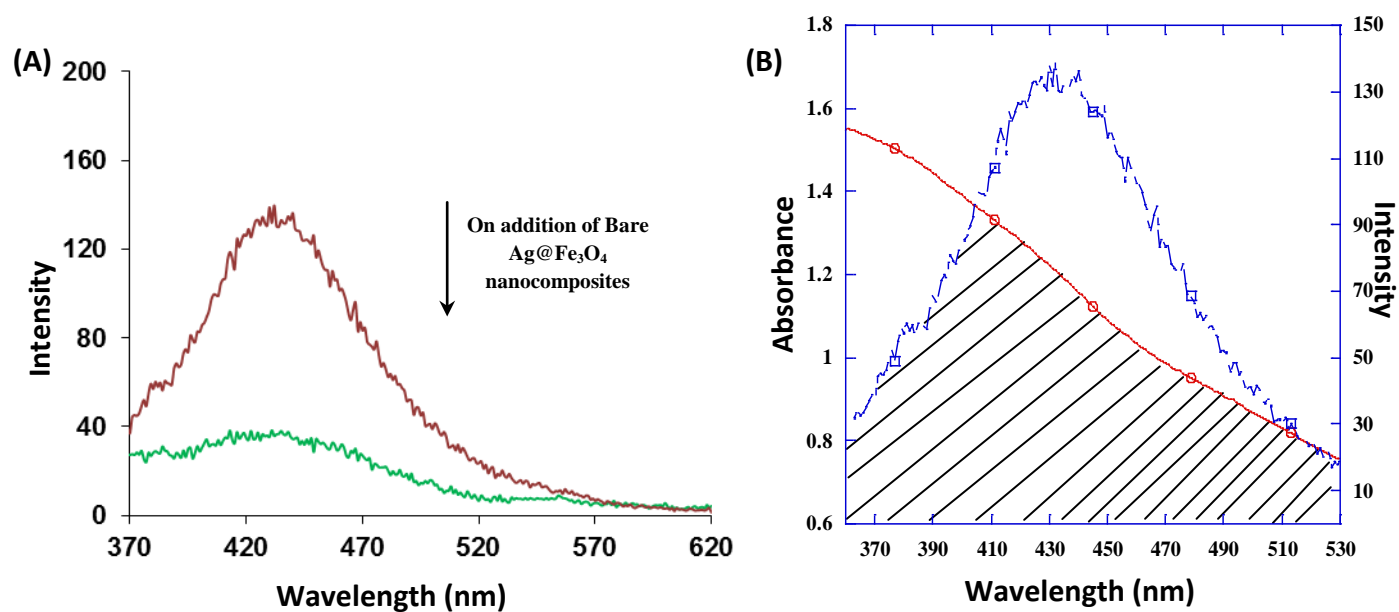


Figure S31 (A) Fluorescence spectra of oxidized species **4** in H₂O-THF (1:1) solvent mixture upon addition of bare Ag@Fe₃O₄ nanocomposites. (B) Spectral overlap of absorption spectrum of Ag@Fe₃O₄ NCs and fluorescence spectrum of oxidized species **4** in H₂O-THF (1:1) mixture showing energy transfer from oxidized species **4** to Ag@Fe₃O₄ NCs.

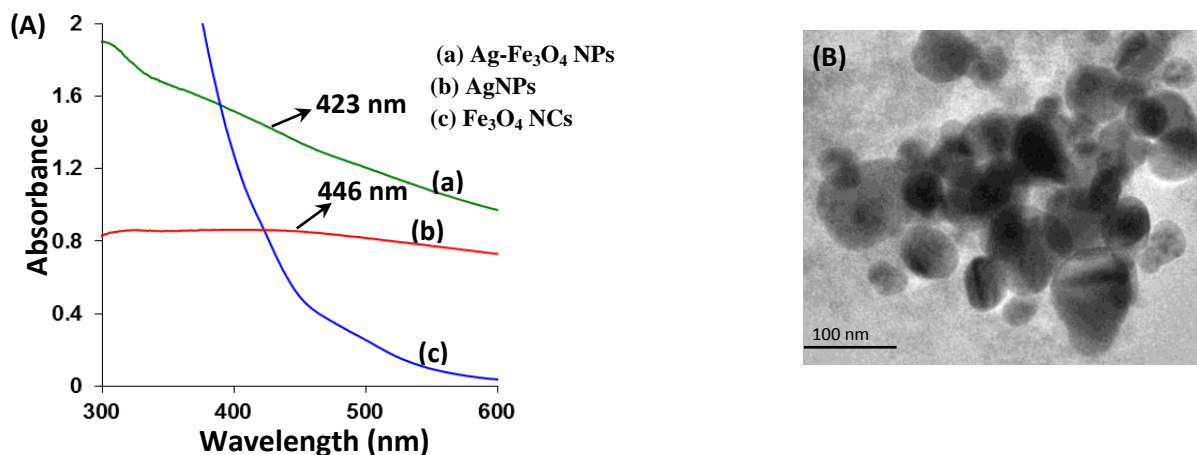
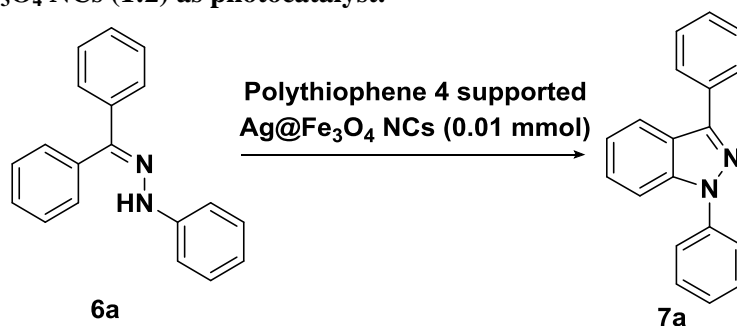


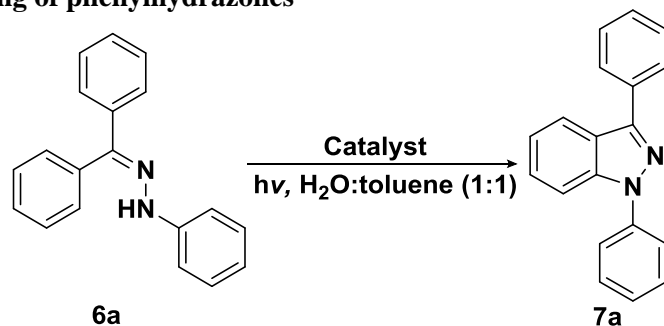
Figure S32 (A) UV-vis spectra of aqueous solution of (a) bimetallic Ag-Fe₃O₄ NPs (b) AgNPs (c) Fe₃O₄ NCs stabilized by assemblies of compound **5**. (B) TEM image of Ag-Fe₃O₄ NPs stabilized by assemblies of compound **5**.

Table S5 Optimization of reaction conditions for dehydrogenative coupling of **6a** utilizing polythiophene **4** supported Ag@Fe₃O₄ NCs (1:2) as photocatalyst.

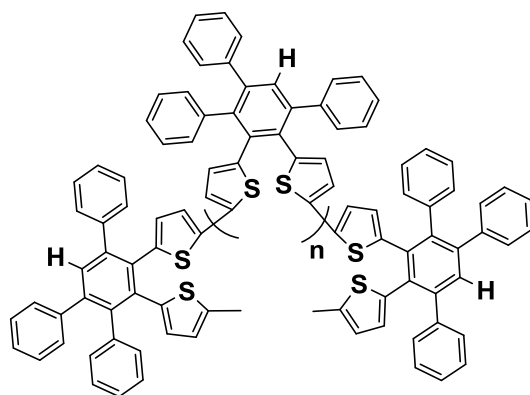


S. No.	Reaction conditions	Time	Yield
1.	Toluene, 110°C	10 h	76%
2.	Toluene:H ₂ O, 110°C	9 h	75%
3.	THF, 50°C	24 h	-
4.	EtOH, 80°C	24 h	-
5.	CH ₃ CN, 80°C	24 h	-
6.	DMSO, 100°C	24 h	25%
7.	1,4-dioxane, 100°C	24 h	30%
8.	Toluene:H ₂ O (1:1), visible light	8h	78%

Table S6 Influence of the stabilizing agent on the photocatalytic efficiency of Ag@Fe₃O₄ nanocomposites in dehydrogenative coupling of phenylhydrazones



S. No.	Catalyst/Reaction Conditions	Time	Yield	BET surface area (in m ² /g)
1.	Polythiophene 4 supported Ag@Fe ₃ O ₄ NCs (1:2), hv	8h	78%	48.18
2.	Polythiophene 4, hv	24 h	-	3.34
3.	Bare AgNPs, hv	24 h	-	2.63
4.	Bare AgNPs + Polythiophene 4, hv	24 h	-	6.12
5.	Bare Fe ₃ O ₄ NCs, hv	24 h	Traces	8.34
6.	Bare Fe ₃ O ₄ NCs + Polythiophene 4, hv	24 h	Traces	16.61
7.	Bare Ag@Fe ₃ O ₄ nanocomposites, hv	24 h	20%	20.30
8.	Bare Ag@Fe ₃ O ₄ nanocomposites + Polythiophene 4, hv	12 h	62%	38.20
9.	Assemblies of compound 5:Ag-Fe ₃ O ₄ , hv	24 h	50%	34.31
10.	Bare Ag@Fe ₃ O ₄ nanocomposites + Polythiophene 8, hv	24 h	22%	22.60
11.	Bare Ag@Fe ₃ O ₄ nanocomposites + Polythiophene 8 + Benzoquinone (1.2 equiv.), hv	24 h	38%	27.01
12.	Polythiophene 4 supported ellipsoidal shaped Ag@Fe ₃ O ₄ NCs (2:1), hv	10 h	67%	42.16



Polythiophene 8

Figure S33 Structure of polythiophene 8.

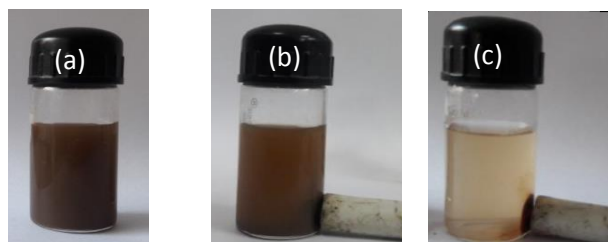


Figure S34 Polythiophene supported Ag@Fe₃O₄ NCs (a) separated aqueous layer after completion of model reaction; (b) a magnetic stirring bar put towards the aqueous layer; (c) an external magnet attracted Ag@Fe₃O₄ NCs.

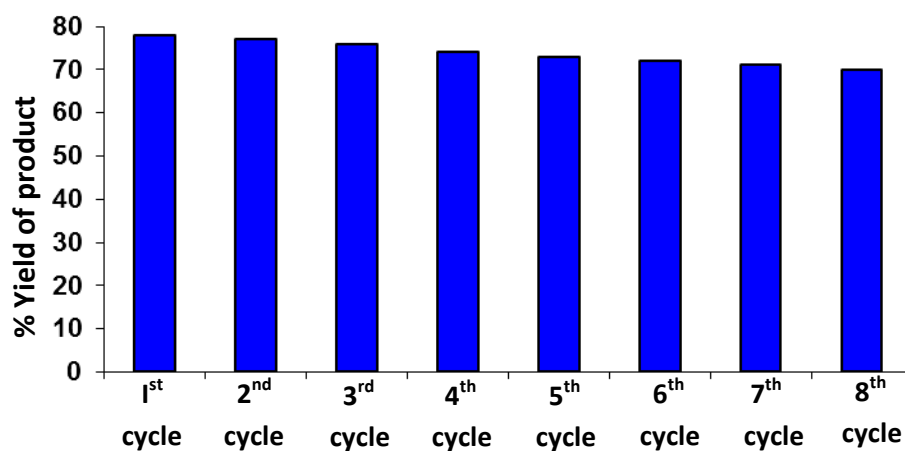
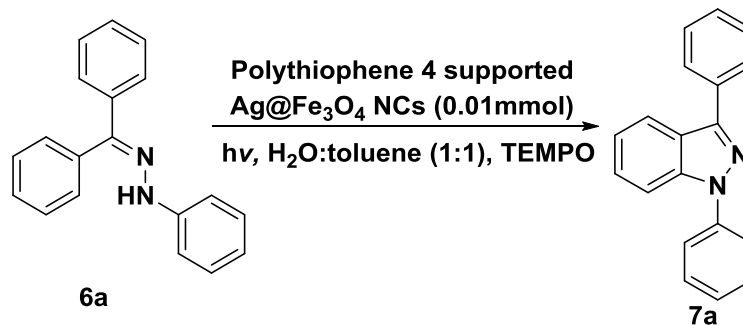


Figure S35 Recyclability of polythiophene **4** supported Ag@Fe₃O₄ NCs as photocatalyst for synthesis of indazole compounds.

Table S7 Effect of addition of TEMPO on dehydrogenative coupling of benzophenone phenylhydrazone, 6a in presence of polythiophene 4 supported Ag@Fe₃O₄ NCs as photocatalyst.



S. No.	TEMPO	Yield of 7a
1.	0 equiv.	78%
2.	1.0 equiv.	46%
3.	2.0 equiv.	15%

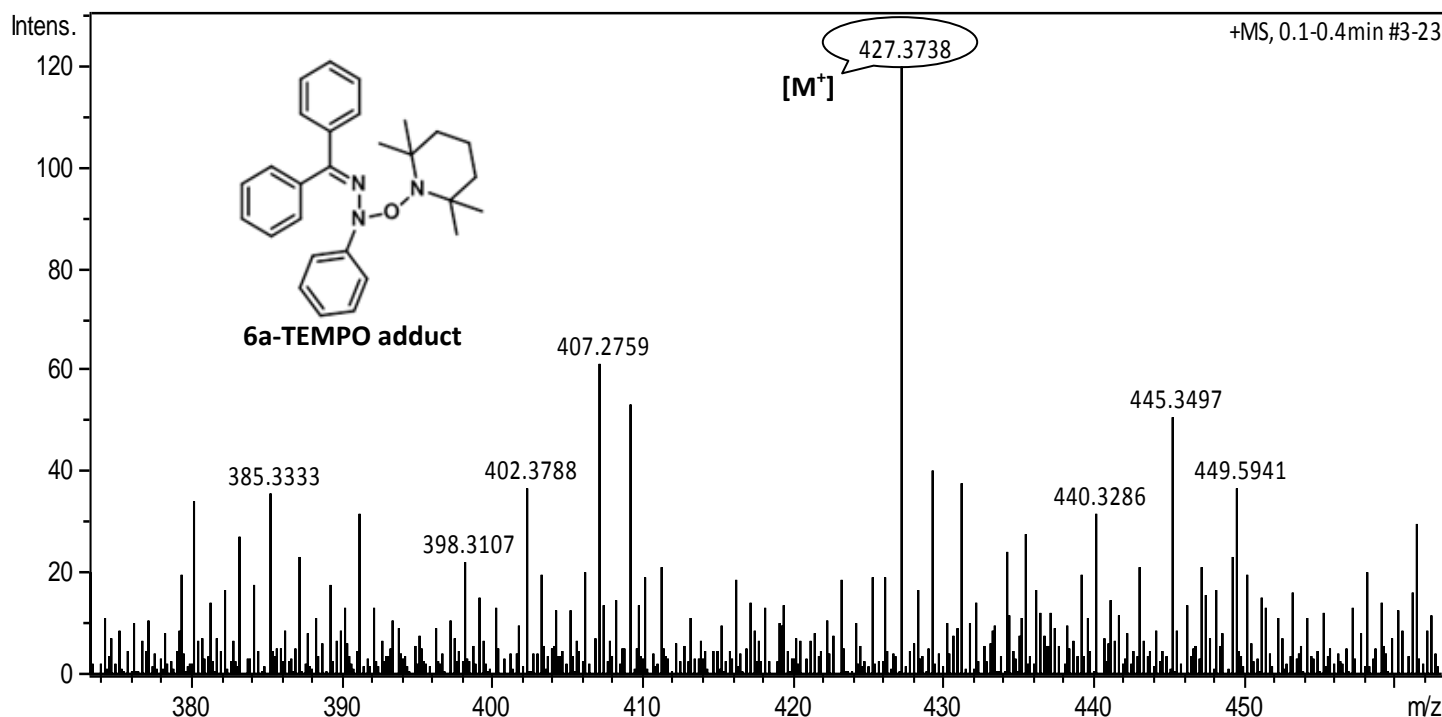
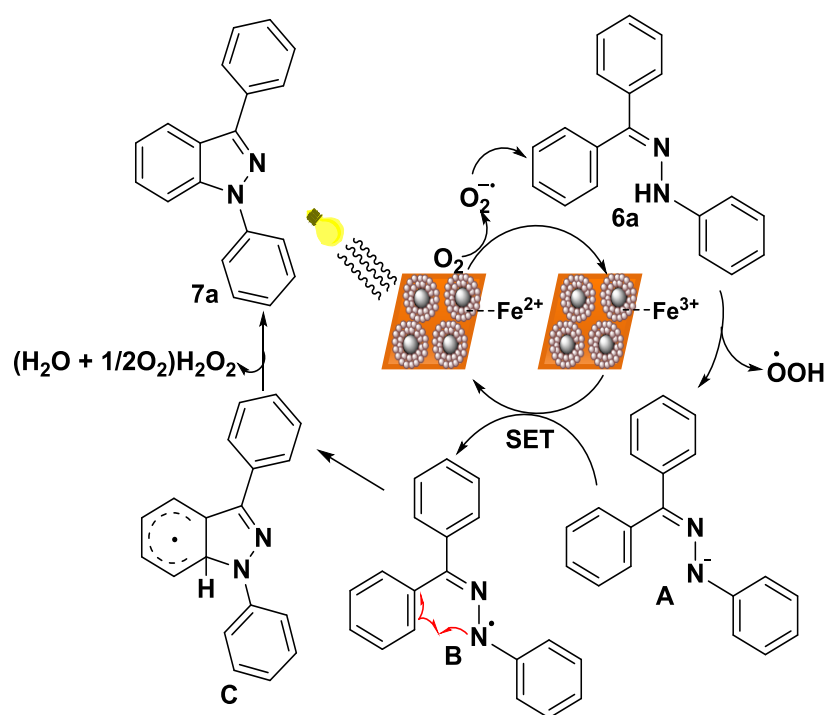


Figure S36 Mass spectrum of 6a-TEMPO adduct



Scheme S4 Plausible mechanism of dehydrogenative coupling of **6a** utilizing polythiophene **4** supported Ag@Fe₃O₄ NCs as photocatalyst

Compound 7a² White solid; 1,3-Diphenyl-1*H*-indazole: (77 mg in 78% yield). ¹H NMR (500 MHz, CDCl₃) δ = 8.10 (d, *J* = 8.0 Hz, 1H), 8.05 (d, *J* = 8.0 Hz, 2H), 7.82-7.79 (m, 3H), 7.58-7.52 (m, 4H), 7.48-7.43 (m, 2H), 7.38 (t, *J* = 7.5 Hz, 1H), 7.30 (t, *J* = 7.5 Hz, 1H) ppm.

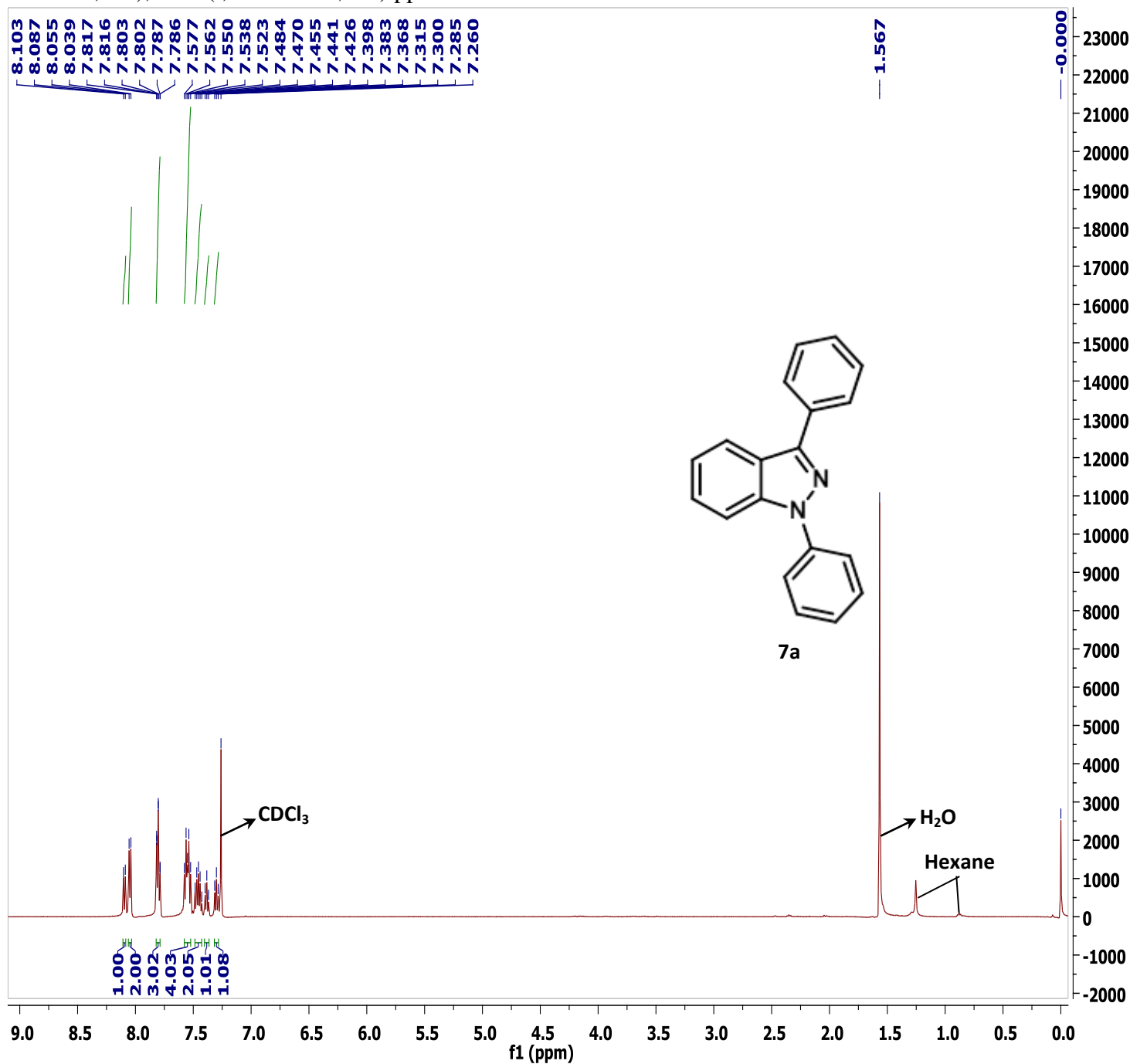


Figure S37 ¹H NMR of compound 7a in CDCl₃

Compound 7b⁹ Gray solid; 3-(4-Fluoro-phenyl)-1-phenyl-1*H*-indazole: (63 mg in 64% yield). ¹H NMR (500 MHz, CDCl₃) δ = 8.04-7.99 (m, 3 H), 7.80-7.78 (m, 3 H), 7.58-7.53 (m, 2 H), 7.49-7.45 (m, 1 H), 7.42-7.37 (m, 1 H), 7.32-7.29 (m, 1 H), 7.24-7.21 (m, 2 H) ppm.

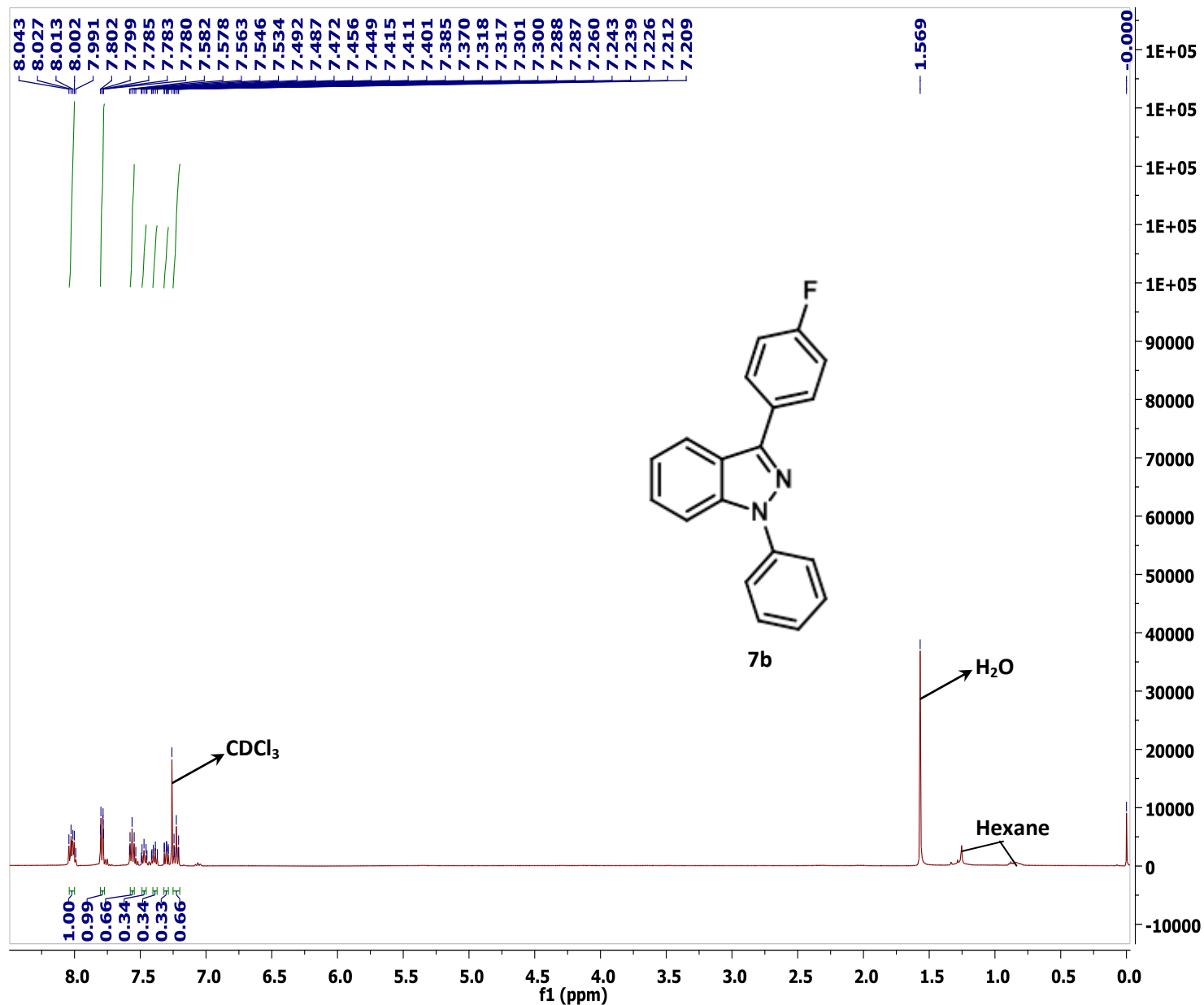


Figure S38 ¹H NMR of compound **7b** in CDCl₃

Compound 7c¹⁰ Pale yellow solid; 3-(4-Chloro-phenyl)-1-phenyl-1*H*-indazole: (65 mg in 66% yield).

¹H NMR (400 MHz, CDCl₃) δ = 8.05 (d, *J* = 8.4 Hz, 1H), 7.99 (d, *J* = 8.4 Hz, 2H), 7.79 (d, *J* = 7.6 Hz, 3 H), 7.57 (t, *J* = 8.0 Hz, 2H), 7.52-7.46 (m, 3H), 7.40 (t, *J* = 7.6 Hz, 1H), 7.31 (t, *J* = 7.6 Hz, 1H) ppm.

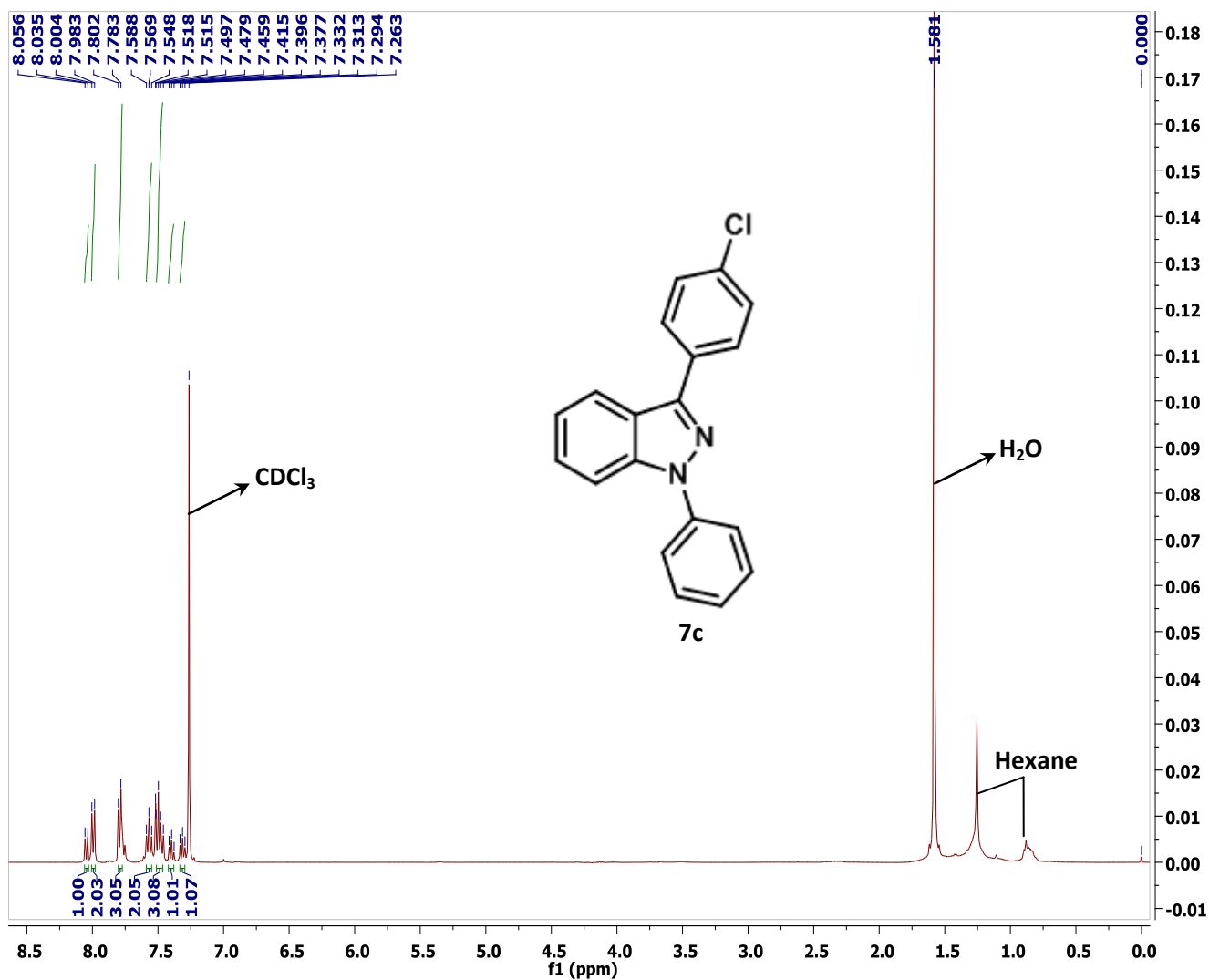


Figure S39 ¹H NMR of compound 7c in CDCl₃

Compound 7d⁹ White solid; 3-(4-Bromo-phenyl)-1-phenyl-1*H*-indazole: (69 mg in 70% yield). ¹H NMR (500 MHz, CDCl₃) δ = 8.05-8.03 (m, 1 H), 7.93 (d, *J* = 8.5 Hz, 2 H), 7.80-7.78 (m, 3 H), 7.66 (d, *J* = 8.5 Hz, 2 H), 7.59-7.55 (m, 2 H), 7.49-7.46 (m, 1 H), 7.41-7.38 (m, 1 H), 7.33-7.29 (m, 1 H) ppm.

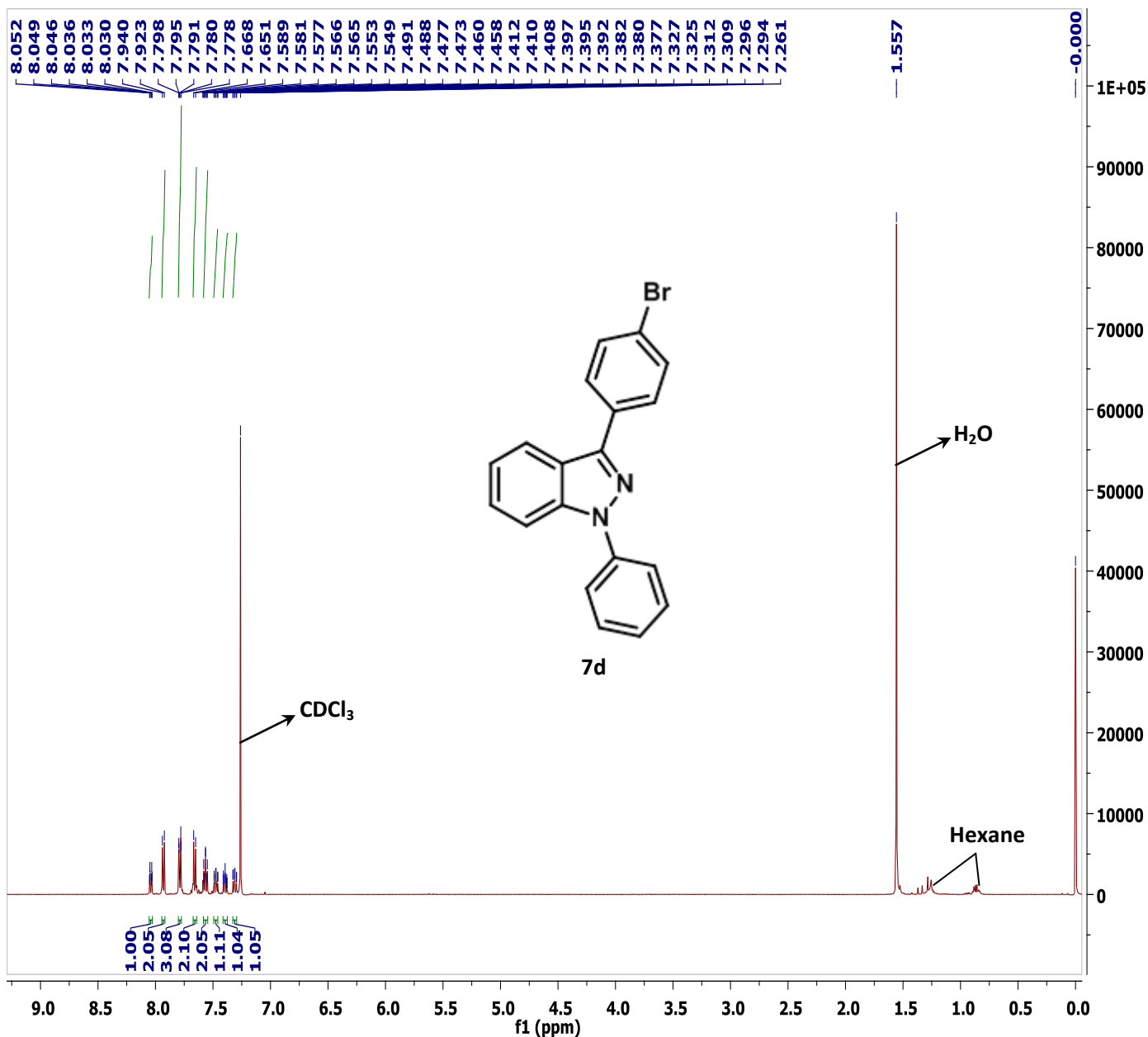


Figure S40 ¹H NMR of compound **7d** in CDCl₃

Compound 7e² Light yellow solid; 6-Fluoro-3-(4-fluoro-phenyl)-1-phenyl-1*H*-indazole: (64 mg in 65% yield). ¹H NMR (500 MHz, CDCl₃) δ = 7.99 -7.94 (m, 3H), 7.75 (d, *J* = 8.0 Hz, 2H), 7.57 (t, *J* = 7.5 Hz, 2H), 7.43-7.39 (m, 2H), 7.23 (t, *J* = 8.8 Hz, 2H), 7.07 (dt, *J* = 9.0, 2.0 Hz, 1H) ppm.

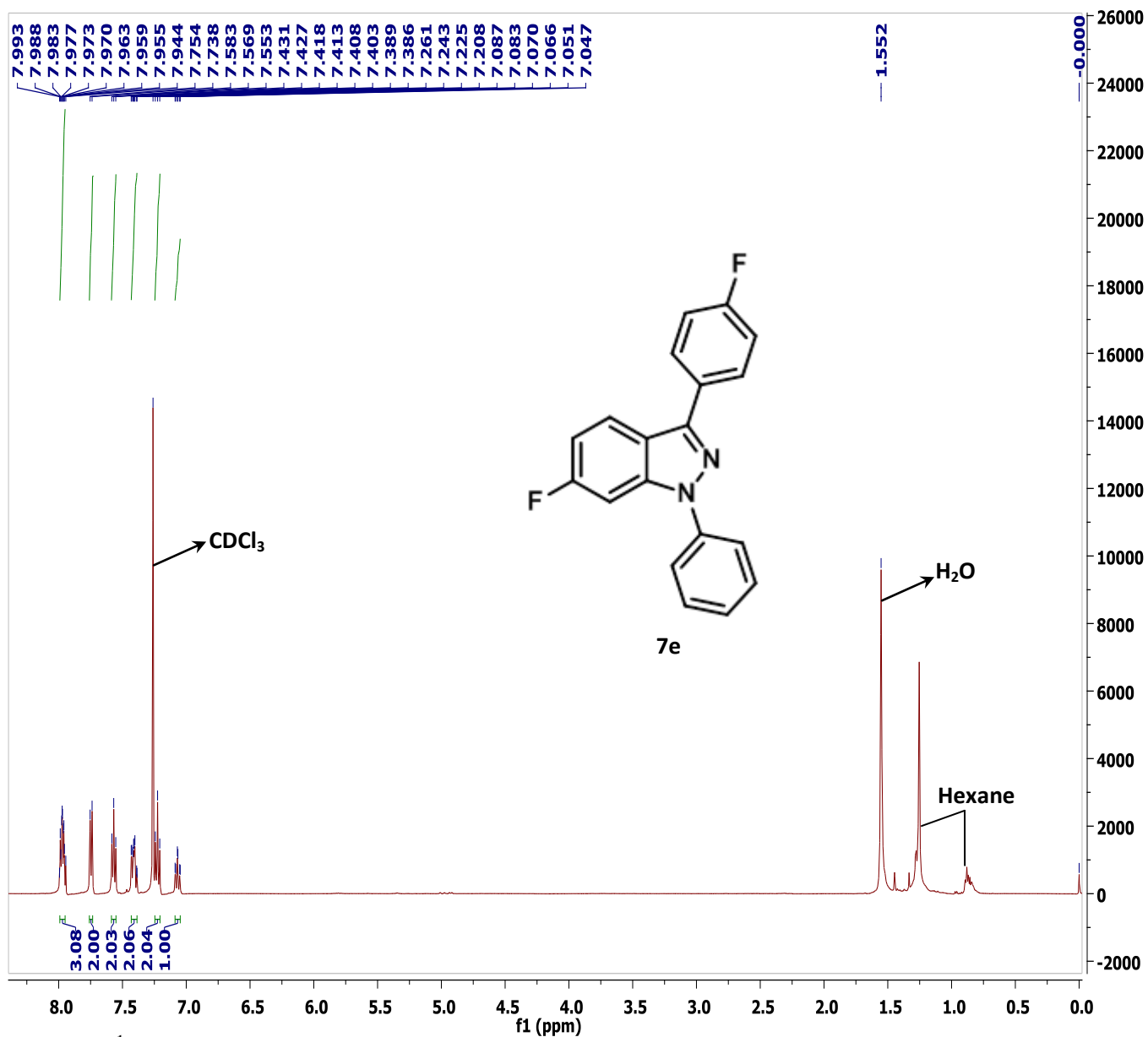
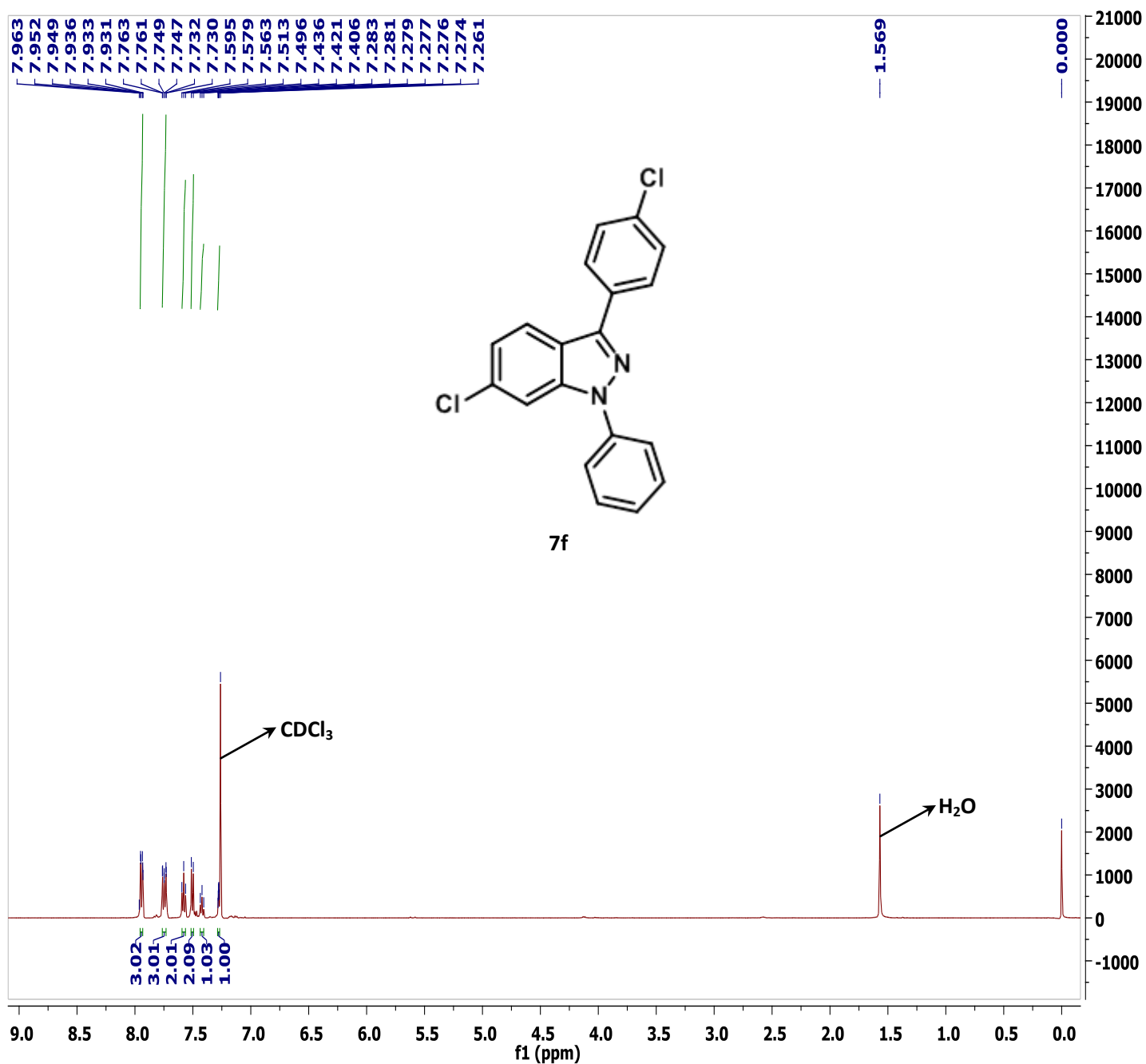


Figure S41 ¹H NMR of compound **7e** in CDCl₃

Compound 7f^{2, 11} White solid; 6-Chloro-3-(4-chloro-phenyl)-1-phenyl-1*H*-indazole: (67 mg in 68% yield).

¹H NMR (500 MHz, CDCl₃) δ = 7.96 -7.93 (m, 3H), 7.76 -7.73 (m, 3H), 7.58 (t, *J* = 8.0 Hz, 2H), 7.50 (d, *J* = 8.5 Hz, 2H), 7.42 (t, *J* = 7.5 Hz, 1H), 7.28-7.27 (m, 1H) ppm.



Compound 7g¹² White solid; 6-Methyl-1-phenyl-3-p-tolyl-1*H*-indazole: (84 mg in 85% yield). ¹H NMR (400 MHz, CDCl₃) δ = 7.96-7.91 (m, 3H), 7.79 (d, *J* = 8.4 Hz, 2H), 7.57-7.51 (m, 3H), 7.38-7.32 (m, 3H), 7.12 (d, *J* = 8.4 Hz, 1H), 2.53 (s, 3H), 2.44 (s, 3H) ppm.

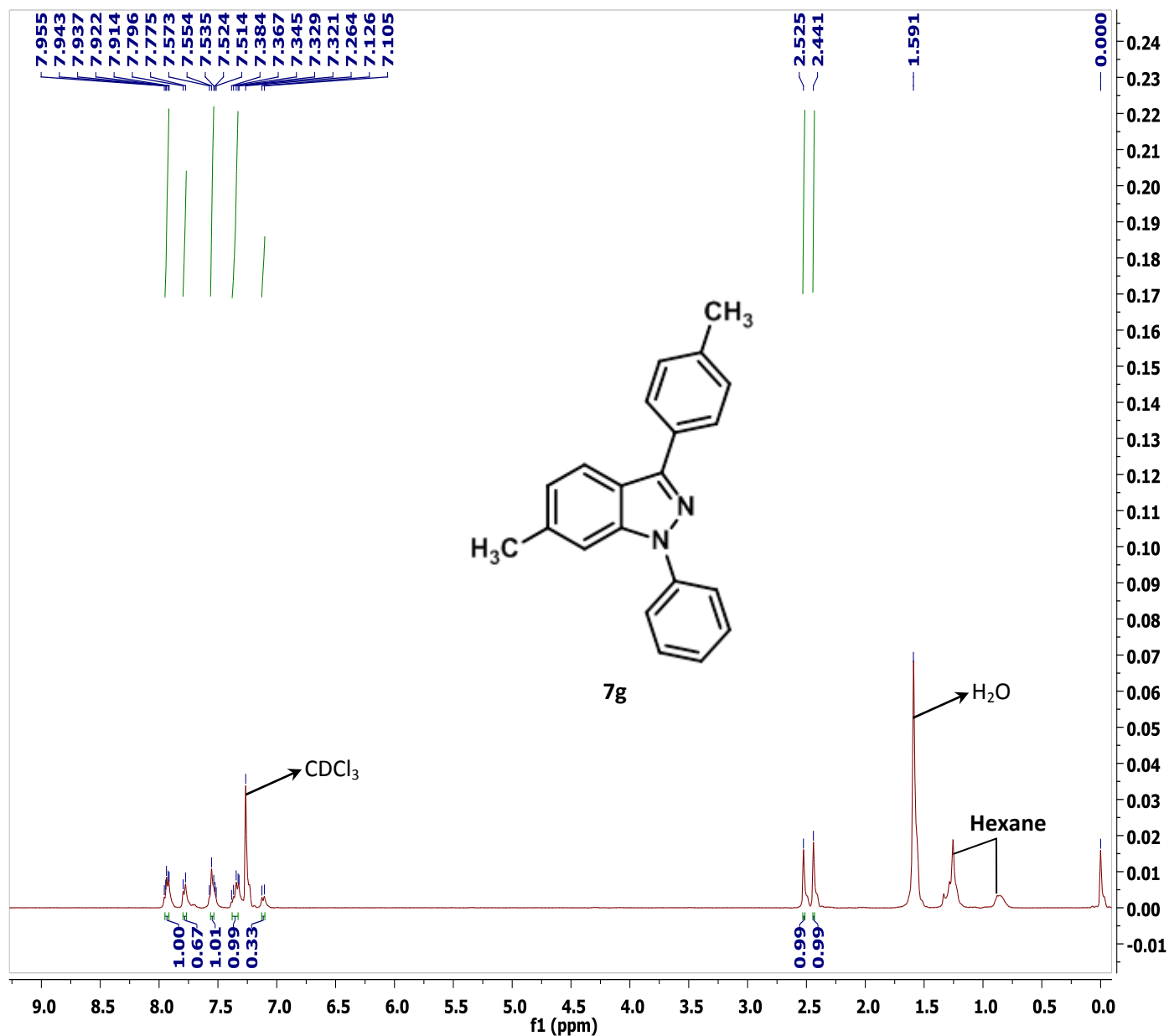


Figure S43 ¹H NMR of compound 7g in CDCl₃

Compound 7h¹¹ Light brown solid; 6-Methoxy-3-(4-methoxy-phenyl)-1-phenyl-1*H*-indazole: (89 mg in 90% yield). ¹H NMR (400 MHz, CDCl₃) δ = 7.94 (d, *J* = 8.8 Hz, 2H), 7.89 (d, *J* = 9.2 Hz, 1H), 7.77 (d, *J* = 7.6 Hz, 2H), 7.55 (t, *J* = 7.6 Hz, 2H), 7.37 (t, *J* = 7.2 Hz, 1H), 7.11 (d, *J* = 2.0 Hz, 1H), 7.05 (d, *J* = 8.8 Hz, 2H), 6.92 (dd, *J* = 8.8, 2.0 Hz, 1H), 3.88 (s, 6H) ppm.

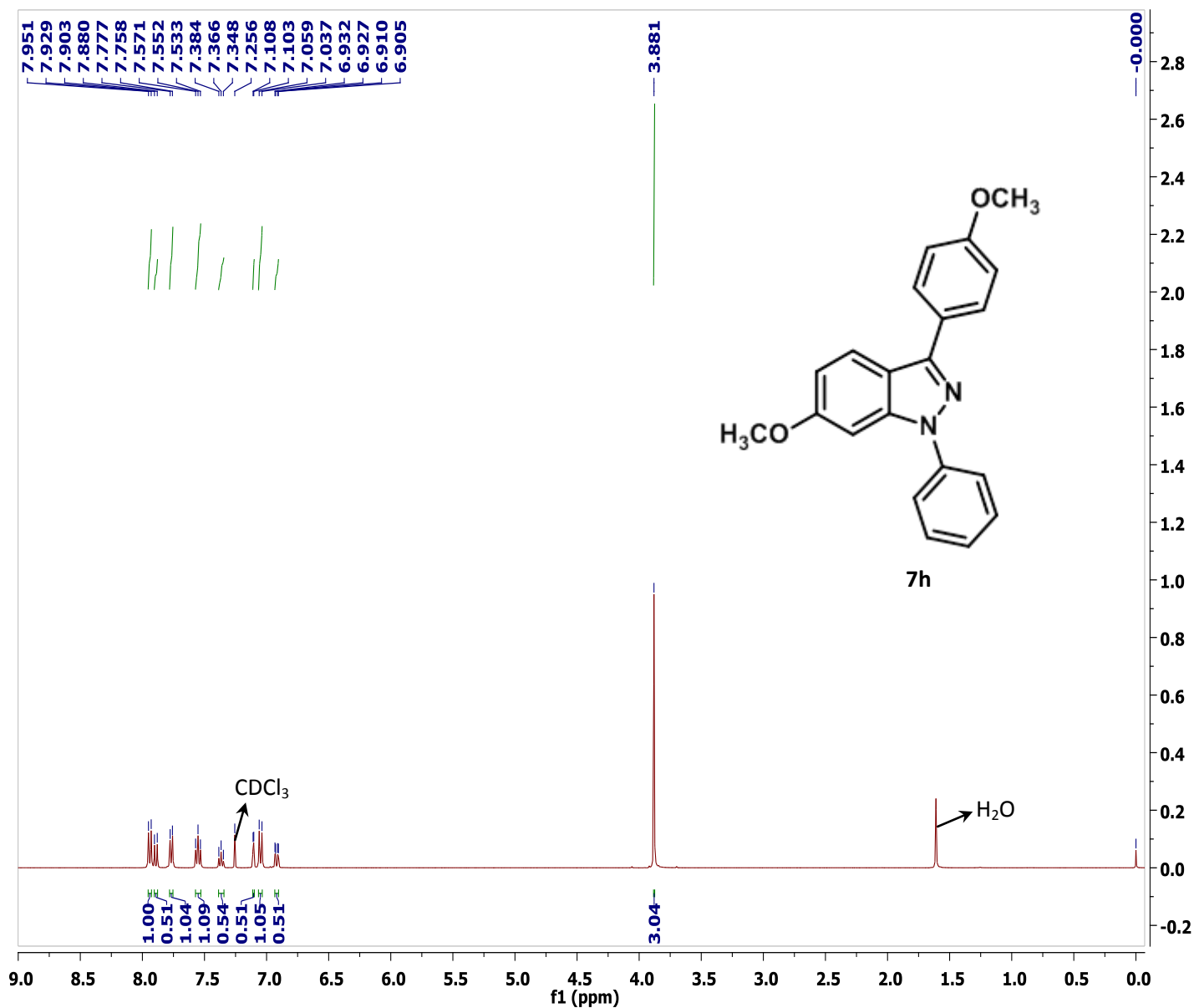


Figure S44 ¹H NMR of compound **7h** in CDCl₃

Compound 7i¹¹ White solid; 1-Phenyl-3-*p*-tolyl-1*H*-indazole: (74 mg in 75% yield). ¹H NMR (500 MHz, CDCl₃) δ = 8.03 (d, *J* = 7.5 Hz, 2H), 7.96 (d, *J* = 8.0 Hz, 1H), 7.79 (d, *J* = 7.5 Hz, 2H), 7.58-7.50 (m, 5H), 7.44-7.35 (m, 2H), 7.13 (d, *J* = 8.5 Hz, 1H), 2.53 (s, 3H) ppm.

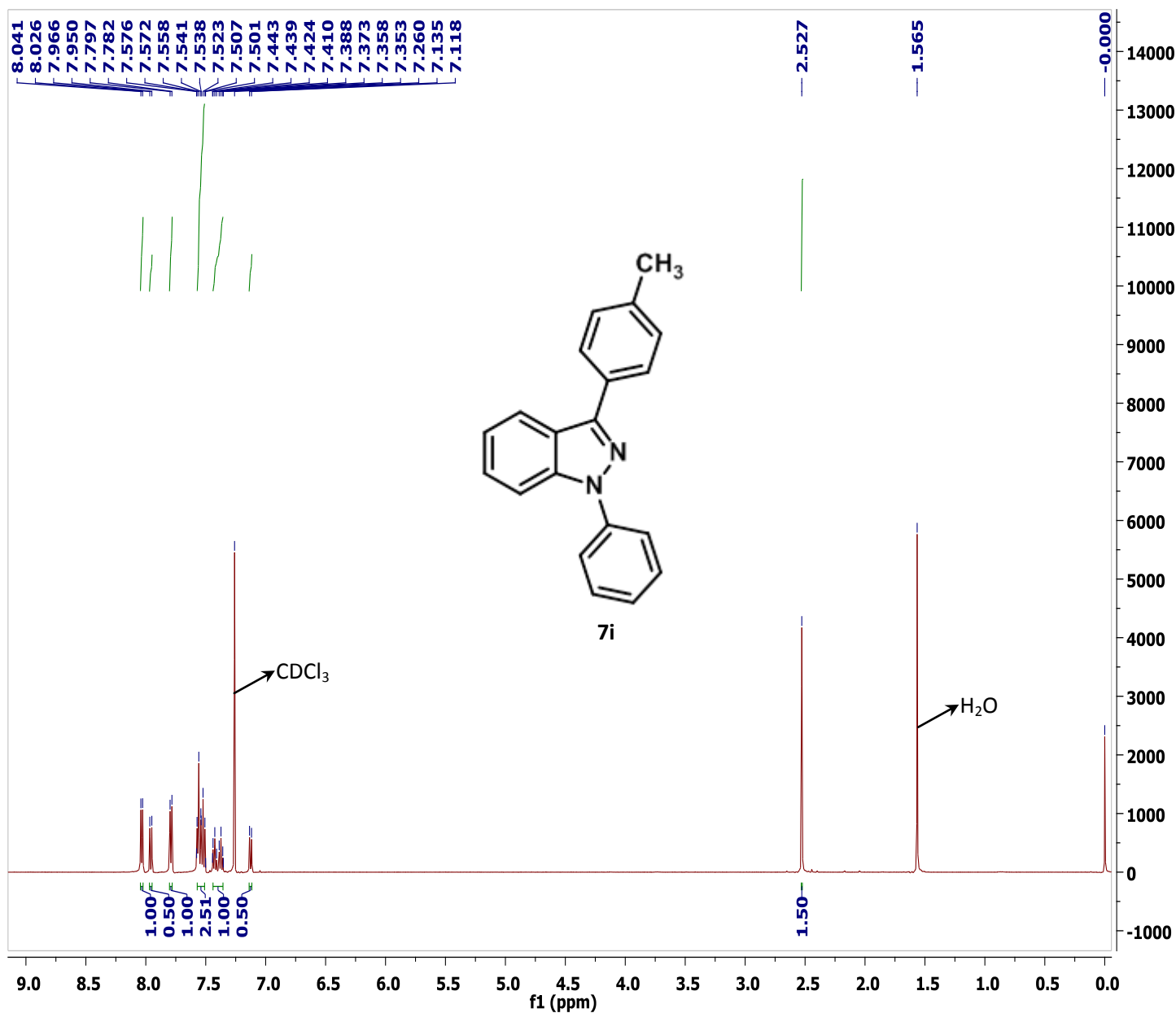


Figure S45 ¹H NMR of compound **7i** in CDCl₃

Compound 7j¹¹ White solid; 6-Methoxy-1,3-diphenyl-1*H*-indazole: (83 mg in 84% yield). ¹H NMR (500 MHz, CDCl₃) δ = 8.01 (d, *J* = 7.5 Hz, 2H), 7.93 (d, *J* = 9.0 Hz, 1H), 7.78 (d, *J* = 8.0 Hz, 2H), 7.58-7.50 (m, 4H), 7.44-7.37 (m, 2H), 7.12 (d, *J* = 2.0 Hz, 1H), 6.94 (dd, *J* = 9.0, 2.0 Hz, 1H), 3.89 (s, 3H) ppm.

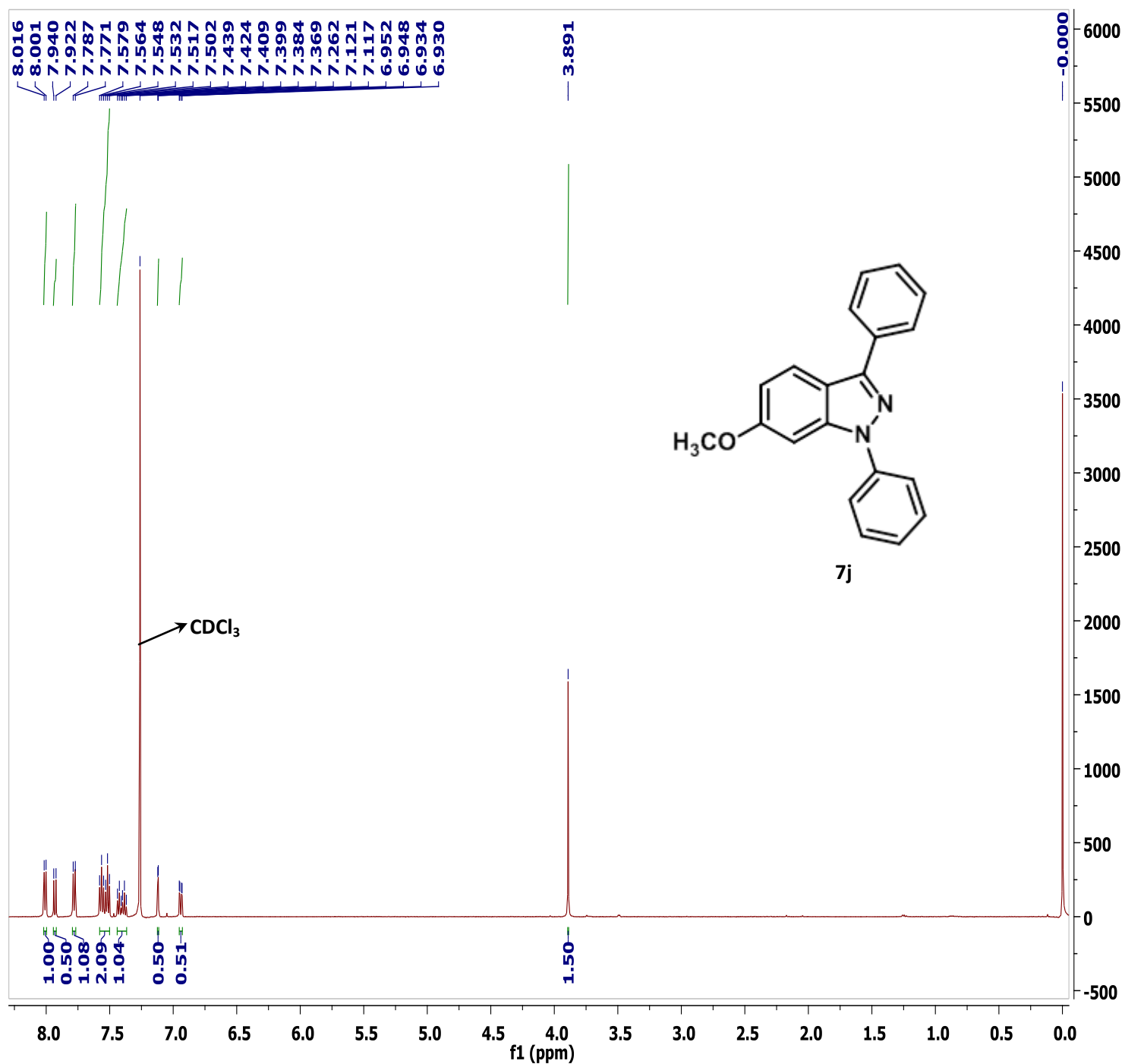


Figure S46 ¹H NMR of compound **7j** in CDCl₃

Compound 3 Yellow solid; mp: >280 °C; (0.18 g in 60% yield). ¹H NMR (500 MHz, CDCl₃) δ = 8.98 (s, 2H), 8.95 (s, 2H), 8.32 (s, 2H), 8.17 (d, *J* = 8.5 Hz, 2H), 7.99 (d, *J* = 8.5 Hz, 2H), 7.74-7.71 (m, 2H), 7.61-7.58 (m, 2H), 7.53-7.50 (m, 2H) ppm.

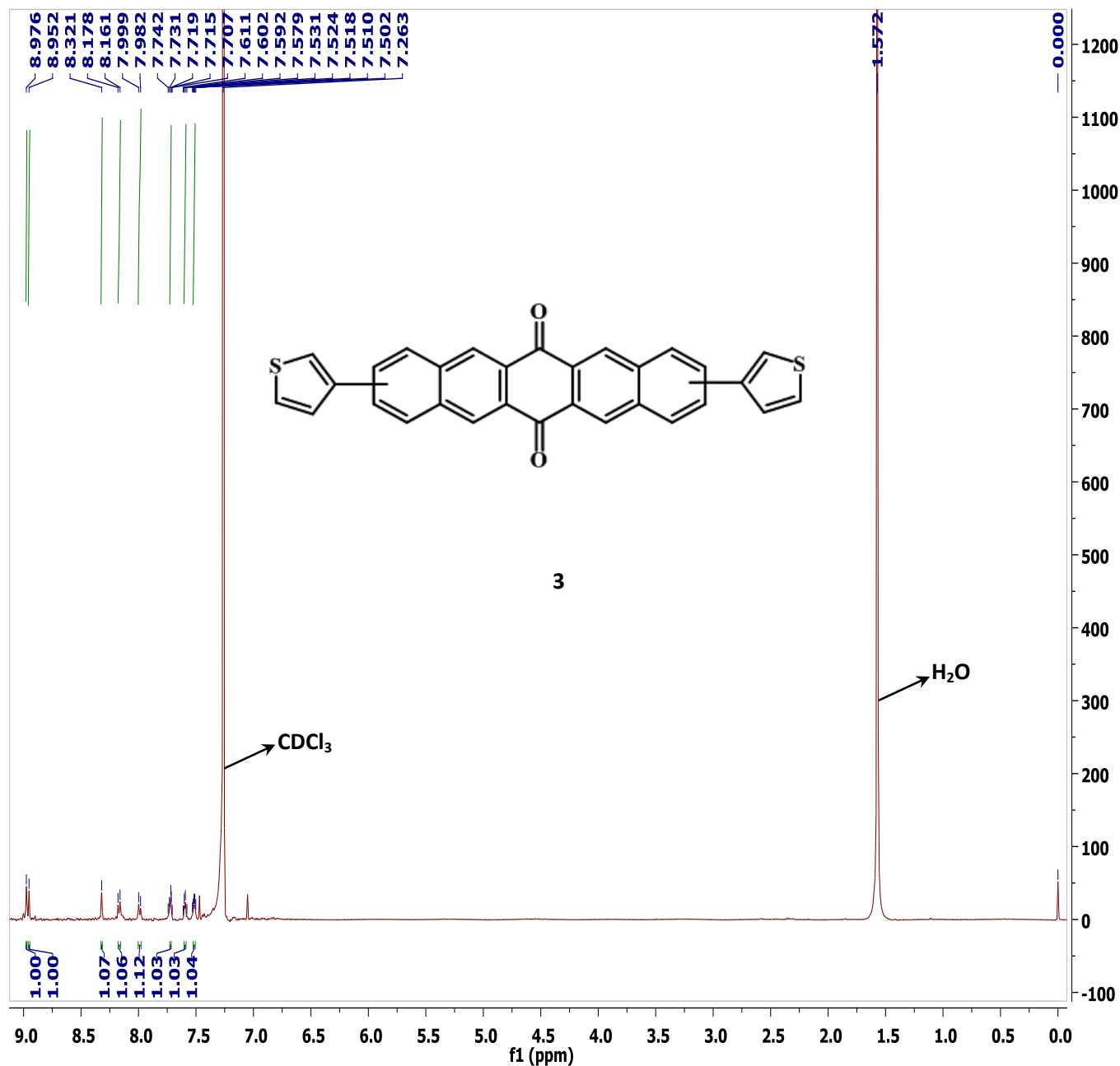


Figure S47 ¹H NMR of compound 3 in CDCl₃

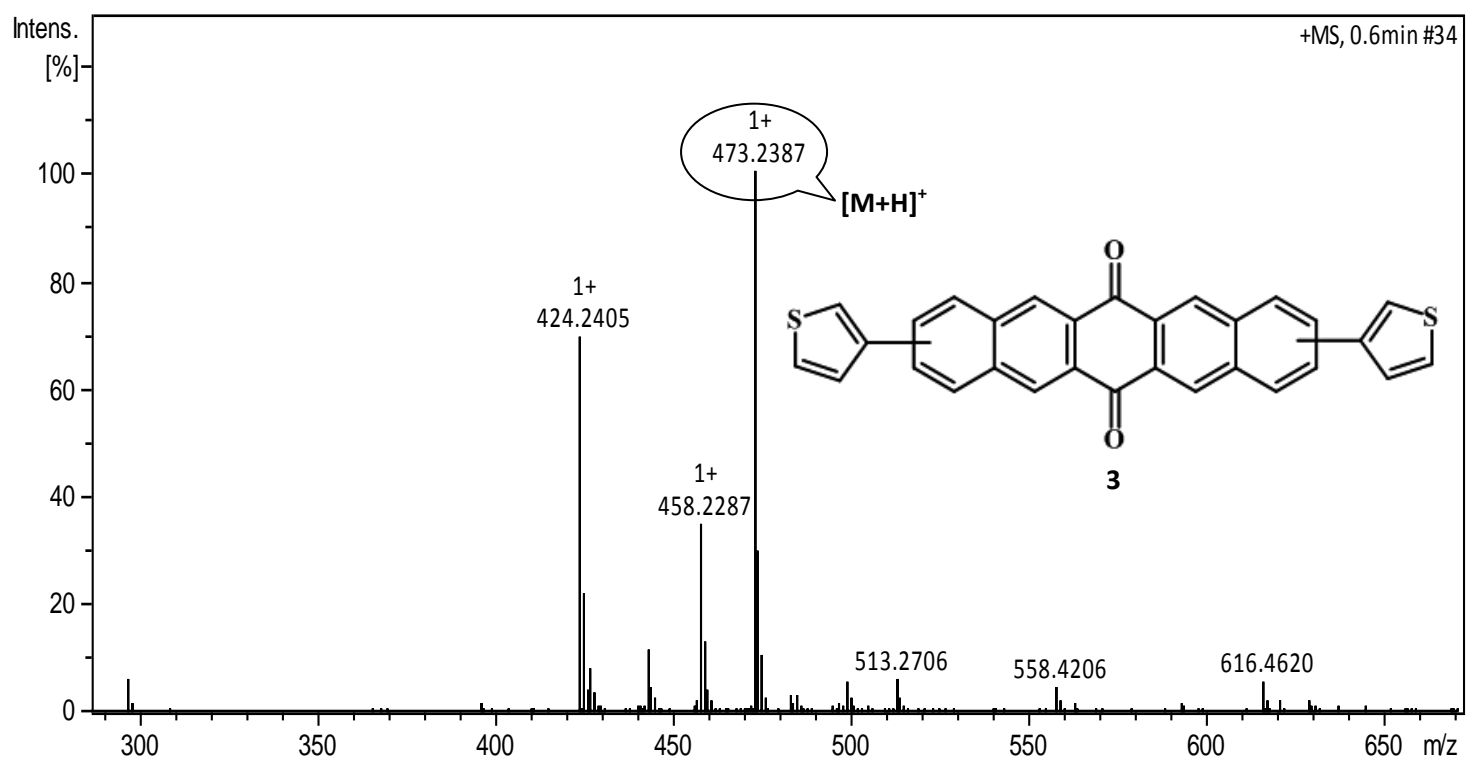


Figure S48 Mass spectra of compound **3**.

Compound 5 Yellow solid; mp: >280 °C; (0.19 g in 63% yield). ^1H NMR (500 MHz, CDCl_3) δ = 8.96 (s, 2H), 8.95 (s, 1H), 8.93 (s, 1H), 8.32 (s, 1H), 8.15-8.13 (m, 3H), 7.99-7.97 (m, 1H), 7.73-7.71 (m, 2H), 7.57-7.56 (m, 1H), 7.44-7.43 (m, 1H), 7.20-7.18 (m, 1H) ppm.

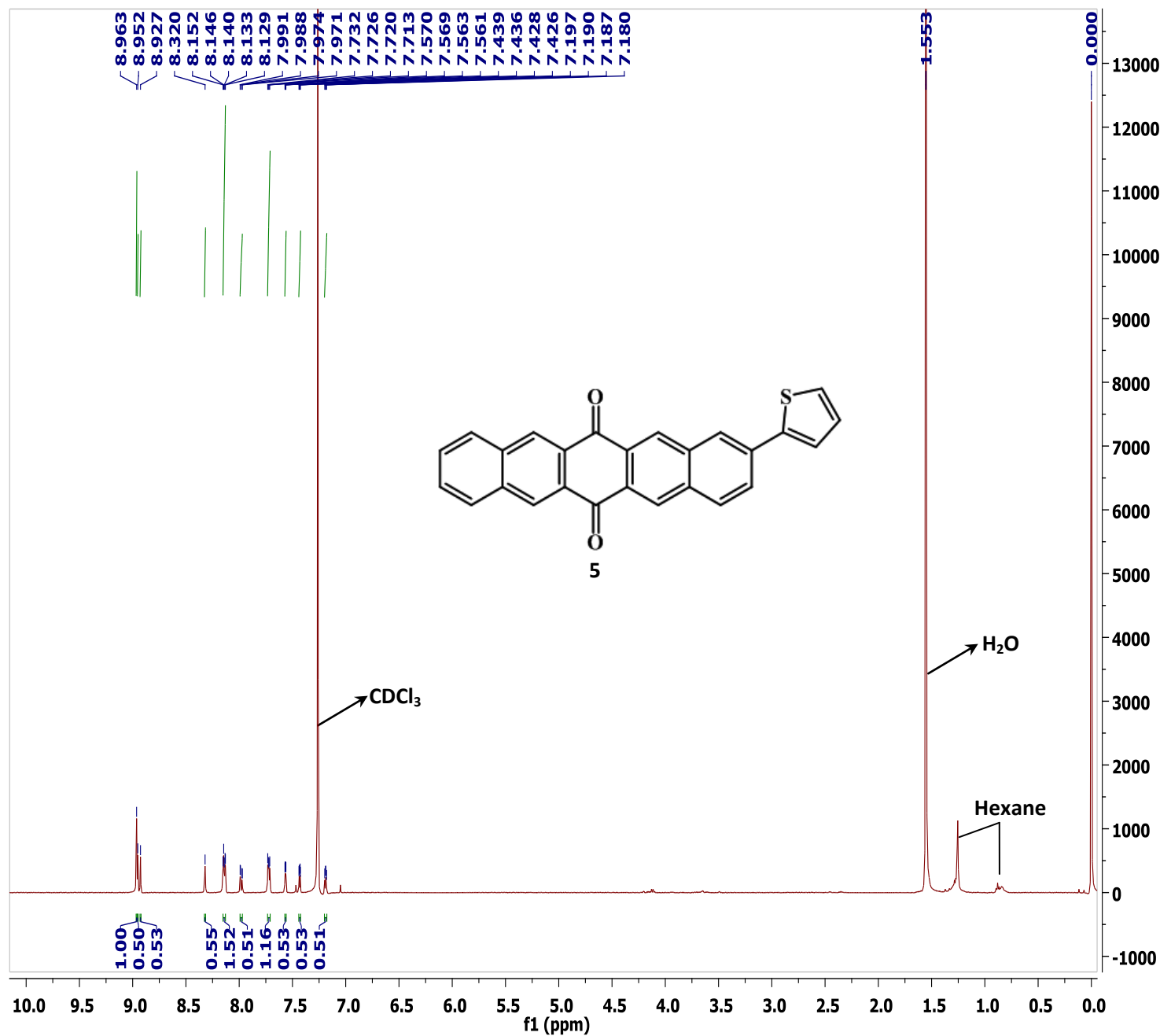


Figure S49 ^1H NMR of compound **5** in CDCl_3

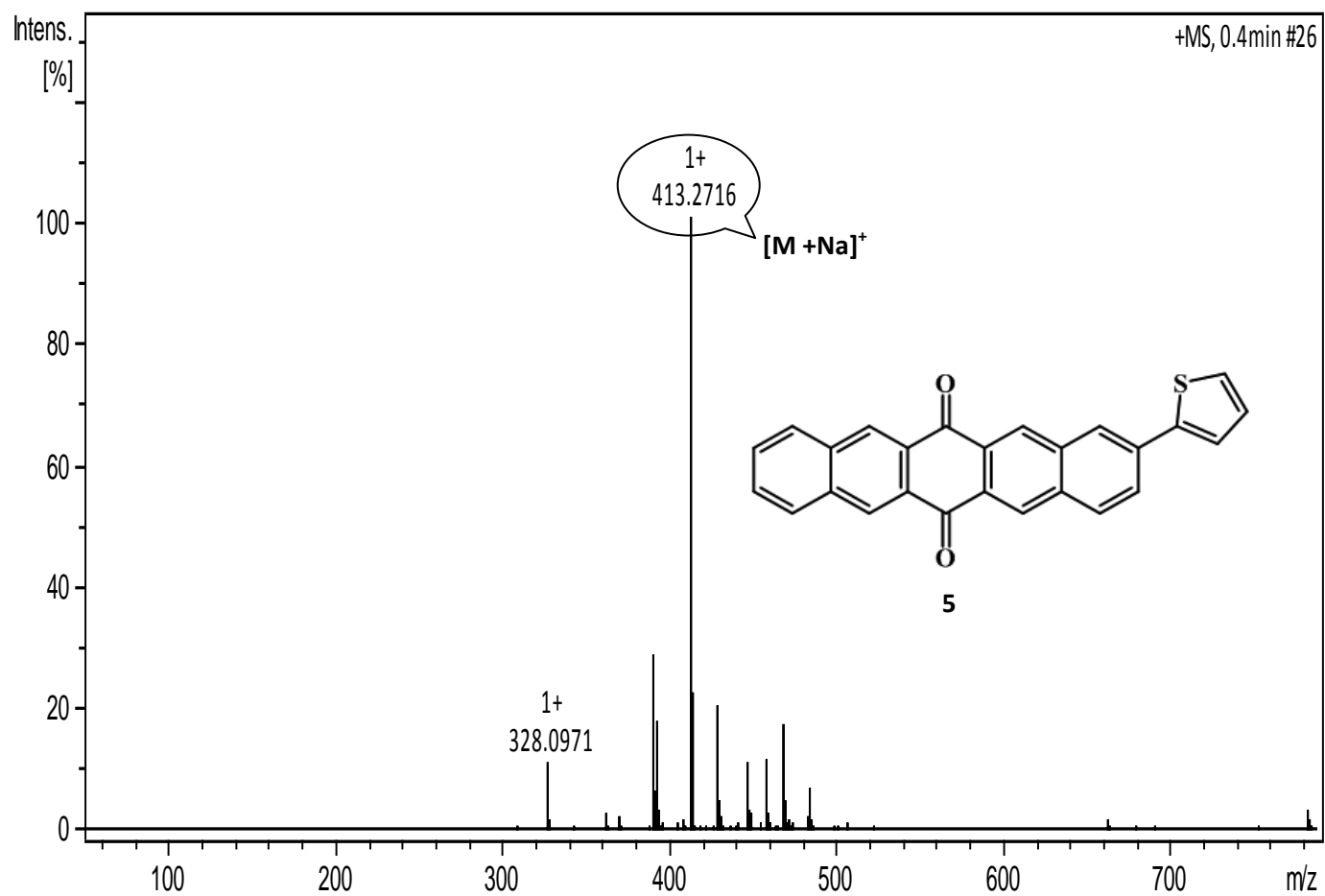


Figure S50 Mass spectrum of compound **5**.

- (1) Chopra, R.; Sharma, K.; Bhalla, V.; Kumar, M. Pentacenequinone-stabilized silver nanoparticles: A reusable catalyst for the Diels-Alder [4 + 2] cycloaddition Reactions. *J. Org. Chem.* **2016**, *81*, 1039-1046.
- (2) Zhang, T.; Bao, W. Synthesis of 1*H*-Indazoles and 1*H*-Pyrazoles via FeBr₃/O₂ mediated intramolecular C-H amination. *J. Org. Chem.* **2013**, *78*, 1317-1322.
- (3) Song, Y.; Tran, V. T.; Lee, J. Tuning plasmon resonance in magnetoplasmonic nanochains by controlling polarization and interparticle distance for simple preparation of optical filters. *ACS Appl. Mater. Interfaces* **2017**, *9*, 24433-24439.
- (4) Fang, W.; Zhang, H.; Wang, X.; Wei, W.; Shen, Y.; Yu, J.; Liang, J.; Zheng, J.; Shen, Y. Facile synthesis of tunable plasmonic silver core/magnetic Fe₃O₄ shell nanoparticles for rapid capture and effective photothermal ablation of bacterial pathogens. *New J. Chem.* **2017**, *41*, 10155-10164.
- (5) Das, R.; Rinaldi-Montes, N.; Alonso, J.; Amghouz, Z.; Garaio, E.; García, J. A.; Gorria, P.; Blanco, J. A.; Phan, M. H.; Srikanth, H. Boosted hyperthermia therapy by combined AC magnetic and photothermal exposures in Ag/Fe₃O₄ nanoflowers. *ACS Appl. Mater. Interfaces* **2016**, *8*, 25162-25169.
- (6) Blocho, M. L.; Paclawski, K.; Wojnicki, M.; Fitzner, K. The kinetics of redox reaction of gold(III) chloride complex ions with L-ascorbic acid. *Inorganica Chimica Acta* **2013**, *395*, 189-196.
- (7) Sau, T. K.; Murphy, C. J. Seeded high yield synthesis of short Au nanorods in aqueous solution. *Langmuir* **2004**, *20*, 6414-6420.
- (8) Goswami, S.; Das, S.; Aich, K.; Sarkar, D.; Mondal, T. K.; Quah, C. K.; Fun, H. K. CHEF induced highly selective and sensitive turn-on fluorogenic and colorimetric sensor for Fe³⁺. *Dalton Trans.* **2013**, *42*, 15113-15119.
- (9) Spiteri, C.; Keeling, S.; Moses, J. E. New synthesis of 1-Substituted-1*H*-indazoles via 1,3-Dipolar Cycloaddition of *in situ* generated nitrile imines and benzyne. *Org. Lett.* **2010**, *12*, 3368-3371.
- (10) Hattori, K.; Yamaguchi, K.; Yamaguchi, J.; Itami, K. Pd- and Cu-catalyzed C-H arylation of indazoles. *Tetrahedron* **2012**, *68*, 7605-7612.
- (11) Kashiwa, M.; Sonoda M.; Tanimori, S. Facile access to 1*H*-Indazoles through iodobenzene-catalyzed C-H amination under Mild, transition-metal-free conditions. *Eur. J. Org. Chem.* **2014**, *22*, 4720-4723.
- (12) Yu, J.; Lim, J. W.; Kim, S. Y.; Kim, J.; Kim, J. N. An efficient transition- metal free synthesis of 1*H*-indazoles from arylhydrazones with montmorillonite K-10 under O₂ atmosphere *Tetrahedron Letters* **2015**, *56*, 1432-1436.